



# **Transportation and deposition of volcanic ash from Iceland to the Arctic**

Josefin Jönsson

20 May 2014

*Josefin Jönsson*

Transportation and deposition of volcanic ash  
from Iceland to the Arctic

Josefin Jönsson

Bachelor report, 15 credits  
Department of Physics  
Lund University, 2014

**Supervisors:**

Jens Havskov Sørensen (Danish Meteorological Institute)  
Ulrik Smith Korsholm (Danish Meteorological Institute)  
Elna Heimdal Nilsson (Lund University)

Department of Physics  
Lund University  
Sölvegatan 14 C  
223 62 Lund

Danish Meteorological Institute, DMI  
Lyngbyvej 100  
2100 København Ø  
Denmark

## **Foreword**

This bachelor thesis is written as part of my bachelor degree in meteorology at Lund University and marks the end of my three years in Lund. The bachelor thesis would not have been the same without the help of my three supervisors, Jens Havskov Sørensen, Ulrik Smith Korsholm and Elna Heimdal Nilsson and I would therefore want to express my great appreciation and gratitude to all three supervisors for all help during the project.

## Table of contents

1. <b>Introduction</b> .....	8
2. <b>Background</b> .....	9
2.1 Volcanoes .....	9
2.2 Grímsvötn and the eruption in 2011 .....	11
2.3 The Arctic and its characteristic atmospheric circulation .....	12
2.4 Transport of particulates to the Arctic .....	13
2.5 Environmental and human effects of volcanic eruptions .....	14
2.6 Aviation and safety concentrations for ash particles .....	15
2.7 The effect of ash particles on snow and ice albedo .....	16
3. <b>Method</b> .....	19
3.1 Dispersion modelling .....	19
3.2 Meteorological data .....	20
4. <b>Result and discussion</b> .....	23
4.1 The 2006 summer scenario .....	24
4.2 The 2014 winter scenario .....	29
4.3 The atmospheric circulation and deposition of ash particles .....	35
4.4 The effect on air traffic .....	36
4.5 The impact on snow and ice albedo .....	36
4.6 Future outlook of Arctic research .....	37
5. <b>Summary</b> .....	39
6. <b>References</b> .....	40
7. <b>Appendix</b> .....	45
7.1 Appendix 1 .....	45
7.2 Appendix 2 .....	46

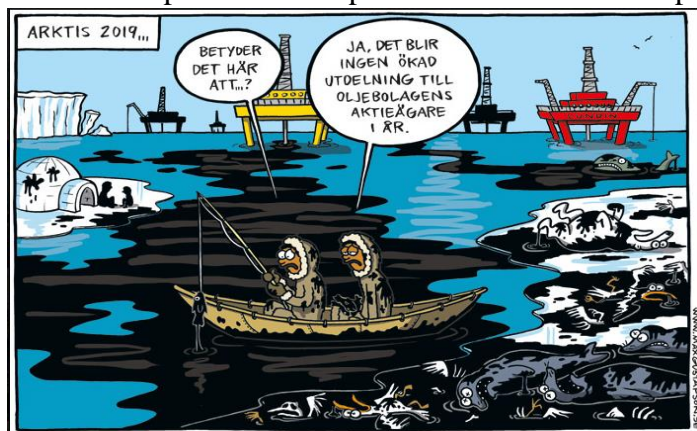
## Den atmosfäriska cirkulationens inverkan på deponering av askpartiklar i Arktis

*Arktis har länge varit ett mysterium på ett flertal sätt för forskare så väl som för gemene man. Då utsträckningen på de väldiga istäckena förväntas minska spås båttrafiken att öka i Arktis, vilket leder till utsläpp av gaser och partiklar som kan påverka miljön. Med de väldiga istäckena och den känsliga miljön kan en ytterst liten förändring i regionen påverka det lokala, regionala och globala klimatet avsevärt så väl kortsiktigt som långsiktigt.*

Det atmosfäriska cirkulationsmönstret i Arktis är beroende av styrkan på hög- och lågtrycken i området samt placeringen av jetströmmen och den arktiska fronten, som skiljer kall luft från den extremt kalla arktiska luften. Dessa fenomen är säsongberoende och varierar i utbredning samt placering under årets alla säsonger, vilket har effekter på den atmosfäriska cirkulationen. Deposition av askpartiklar på is- och snöytor förändrar strålningsupptaget från solen, vilket leder till en ökad upptagning av strålning och därmed en minskning i mängden snö och is. Så väl som att påverka istäcket ger askpartiklarna konsekvenser för människor och djur genom att skapa irritation i ögon, andningsorgan och kan i värsta fall leda till döden. De vulkaniska askpartiklarna utgör även en oerhörd risk för flygplan, då partiklarna skapar ett tunt lager av vulkaniskt glas i jetmotorn som på grund av detta slutar fungera normalt.

Syftet med kandidatarbetet är att illustrera och reda ut en del av dessa frågetecken gällande den potentiellt säsongbaserade atmosfäriska cirkulationen till Arktis och effekterna av deposition av askpartiklar på de väldiga istäckena i Arktis. Påverkan på flygtrafiken utav askpartiklar i luften studeras också och värderingar utifrån de gällande gränsvärdena görs med avseende på flygförhållandena.

Arbetet utförs med hjälp av programmet ”Danish Emergency Response Model of the Atmosphere” (DERMA) som simulerar det vulkaniska utbrottet av den isländska vulkanen Grímsvötn år 2011 i olika vädersituationer. Utbrottet av den isländska vulkanen Grímsvötn varade i sju dagar och askplymen nådde som högst 15 km upp i luften. För att illustrera en säsongbaserad cirkulation studeras ett sommarfall år 2006 och ett vinterfall år 2014. Resultatet visar en signifikant skillnad i deposition och transport av vulkanisk aska mellan de två vädersituationerna. I sommarsituationen sker transporten och depositionen främst i Europa och Medelhavsområdet medan vintersituationen domineras av transport av vulkanaska norröver till Arktis. Depositionen som sker under vintern i Arktis är avsevärt mindre än depositionen under sommaren i Europa och Medelhavsområdet, vilket är ett resultat av de olika meteorologiska egenskaper som är typiska för områdena.



*Figur 1. En ökad transport och utvinning i Arktis kan påverka den känsliga miljön på ett flertal sätt (Gustafson, 2011).*

Täcket av aska som lägger sig på den arktiska isen är dock så tunt att det troligtvis inte har någon påverkan på det kort- eller långsiktiga klimatet, men då forskningen för sådana tunna asktäcken är bristande bör det utföras mer forskning om detta i framtiden för att med absolut säkerhet hävda detta. Mängden askpartiklar i luften utgör inte några större problem för flygtrafiken, men förseningar kan förväntas.

Avslutningsvis kan slutsatsen dras att de två situationerna som studerades illustrerar en säsongsbetonad atmosfärisk cirkulation, där depositionen är beroende av säsong, men för att bekräfta en sådan trend bör flertalet situationer analyseras och granskas.

**Handledare:** Jens Havskov Sørensen, Ulrik Smith Korsholm och Elna Heimdal Nilsson  
Examensarbete 15 hp i Fysik (Meteorologi) 2014  
Fysiska institutionen, Lunds universitet  
Danmarks Meteorologiska Institut (DMI)

## Abstract

As the Arctic will become more available to shipping traffic in the future, given the current trend of diminishing ice sheets continues, the emission of particles and gases originating from ships will increase in the Arctic. The emission of particles and gases can affect the sensitive Arctic environment in many ways, e.g. change albedo by deposition, affect air traffic, harm livestock and humans etc. Therefore it is of interest to explore the seasonal effect on the atmospheric circulation and dispersion of particles to the Arctic. The concentration and deposition of volcanic ash particles with regard to air traffic is also explored. The dispersion and deposition is explored by studying dispersion and deposition of volcanic ash in the programme “Danish Emergency Response Model of the Atmosphere” (DERMA) in operation at the Danish Meteorological Institute (DMI). The result shows a winter season that is characterized by dispersion and deposition of particles into the Arctic, while the summer season has little or no dispersion or deposition into the Arctic. In summer, Europe receives the largest deposition of particles ( $1 \text{ g/m}^2$ ) while the Arctic receives the largest amount of ash particles in the winter ( $> 1 \text{ g/m}^2$ ). The deposition of ash particles in the Arctic creates a very thin layer of ash particles that most likely does not affect the albedo of the ice and snow-covered surface. Therefore the short- and long-term climate effects are not significant. The effect of ash particles on air traffic is minor and the area affected shifts depending on the season due to the difference in dispersion. The major impact on air traffic is most likely delays of some departures. However, it is important to keep in mind that to fully prove a seasonal difference in dispersion and deposition, a more detailed and precise investigation needs to be carried out with statistics of the different seasons.

**Keywords:** *Grímsvötn 2011, volcanic eruption, the Arctic, transportation and deposition of volcanic ash, albedo, air traffic.*

## **1. Introduction**

As the area and thickness of the sea ice in the Arctic has decreased during the past decades, the Arctic has become more available to shipping traffic and to the exploration of its enormous resources, e.g. oil, gas, minerals and fishery (ACIA, 2005). Assuming that the current trend continues, the probable increase in shipping traffic in and to the Arctic will lead to emission of particles and gases that will circulate and deposit in the Arctic, affecting the sensitive Arctic environment (ACIA, 2005; Arctic Council, 2009). The transport pathways and patterns in the Arctic circulation are not yet fully described and more research needs to be carried out to fully grasp the atmospheric circulation patterns in the Arctic.

As a result of this lack of knowledge, the purpose of this bachelor project is to explore the atmospheric circulation in the Arctic and illustrate its seasonality. The atmospheric circulation patterns are investigated by observing the transportation and deposition of volcanic ash from Iceland to the Arctic using the 2011 Grímsvötn eruption as ash release scenario for the chosen meteorological cases. The emission of ash particles during Icelandic eruptions is of interest, since the particles can be hazardous to humans and livestock and have the potential to cause short-term climate changes in the Arctic, affect land-based and marine ecosystems and disrupt air traffic (Durant et al., 2010; Niemeier, 2009). Iceland, which is located close to the Arctic, experiences strong variations in transport pathways on a seasonal basis with consequences for ash dispersion (Quinn, 2011).

The Danish Emergency Response Model of the Atmosphere (DERMA) will be used to simulate volcanic eruptions of ash in different weather situations characteristic of two seasons, summer and winter. An attempt to illustrate the general transportation and deposition of ash in summer and winter will be made for the Arctic, as well as the transport pathways of interest to air traffic and the effect on albedo as a result of deposition of ash particles.



## **2. Background**

### **2.1 Volcanoes**

In the following section the general properties of volcanoes will be described, as well as the processes that follow a volcanic eruption. Volcanic activity is often linked to plate tectonics and most volcanoes are therefore located near plate boundaries (Keller and DeVecchio, 2012). When lithospheric plates spread or sink at plate boundaries, they interact with materials in the earth and produce molten rock, called magma when it is inside the Earth and lava when the volcano erupts it onto the surface of the Earth (Keller and DeVecchio, 2012).

There are several types of volcanoes, e.g. shield-, composite- (strato) and dome volcanoes (Keller and DeVecchio, 2012). Grímsvötn, located on Iceland, is an example of a so called stratovolcano. The magma from stratovolcanoes is in general more viscous and has a higher volatile content compared to shield volcanoes; however it is less viscous and volatile compared to dome volcanoes (Keller and DeVecchio, 2012). Stratovolcanoes are able to erupt many different variations of lava, e.g. basalt or intermediate forms between andesite and rhyolite (Keller and DeVecchio, 2012).

During a volcanic eruption pyroclastic activity can take place, meaning that tephra is erupted from a volcanic vent into the atmosphere (Keller and DeVecchio, 2012). Tephra is a collective name for all types of volcanic materials that are erupted from a volcano during an eruption. Tephra particles span over a size range of several orders of magnitude and the finest particles are fine dust followed by sand-sized ash particles less than 2 mm (Keller and DeVecchio, 2012). The particles coming next in size is small gravel-sized lapilli between 2 to 64 mm, followed by large angular blocks and smooth-surfaced bombs larger than 64 mm (Keller and DeVecchio, 2012). When tephra accumulates it produces a pyroclastic deposition on the surface.

The volcanic ash that is emitted during a volcanic eruption can cover vast areas, e.g. continents, and be hazardous (Keller and DeVecchio, 2012). Vegetation, including crops and trees, can be destroyed by volcanic eruptions and the following deposition of ash. Surface water can be contaminated by sedimentation and the fine ash particles can clog the gills of fish and kill other types of aquatic life (Keller and DeVecchio, 2012). Ash particles often have a chemical coating that may produce a momentary increase in the water's acidity (Keller and DeVecchio, 2012). Deposition of ash particles upon structural buildings also pose a threat, since only 1 cm of ash upon a 140 m<sup>2</sup> roof adds an extra 2.5 tons of weight (Keller and DeVecchio, 2012). Ash particles also pose as a health hazard for humans by irritation of the respiratory system and eyes (Keller and DeVecchio, 2012). Volcanic ash poses a large threat to air traffic since the melted silica-rich ash forms a thin layer of volcanic glass in the jet engines, which might malfunction as a result (Keller and DeVecchio, 2012).

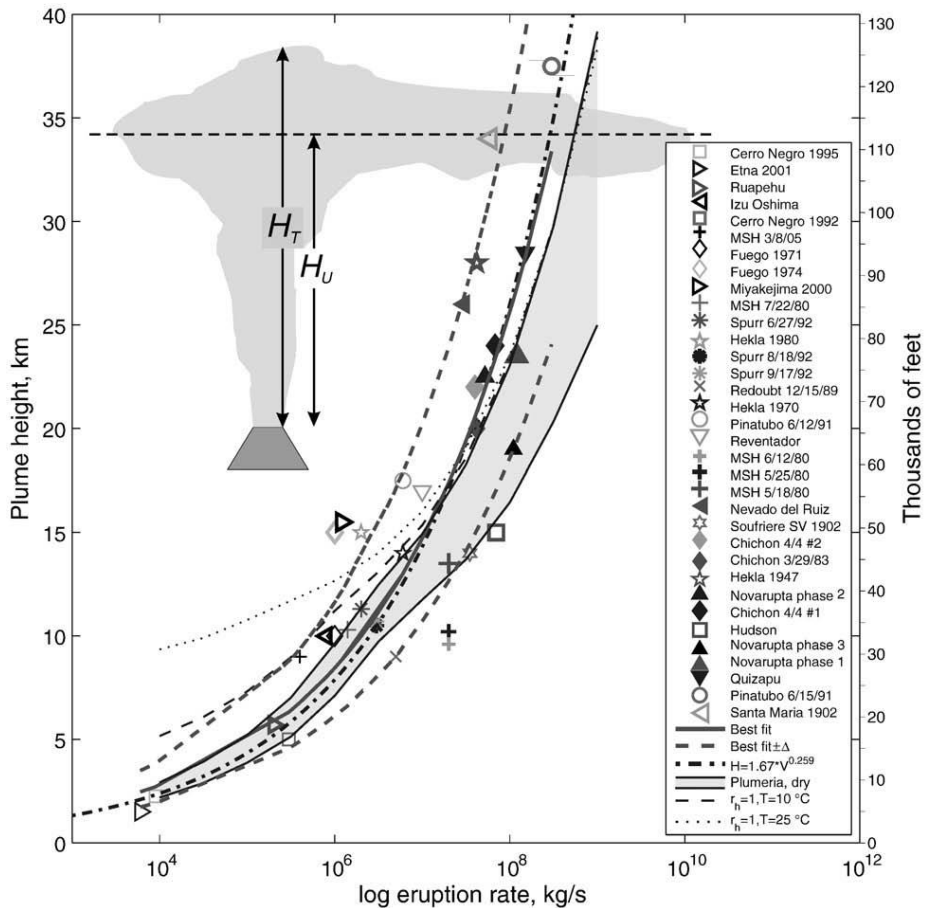


**Figure 2.** The relationship between plume height,  $H$ , in kilometres and eruption rate in kg per second (Mastin et al., 2009). The plume height,  $H$ , is divided into  $H_u$ , the height at the center of the umbrella cloud and  $H_T$ , the top of the ash plume. The legend contains symbols for each studied volcanic eruption and the bold solid line corresponds to the best fit to the data.

Volcanic eruptions that are a threat to the environment, as well as to air traffic, differ greatly in size and style (Mastin et al., 2009). A common trait for volcanic eruptions is an increase in plume height above the volcano,  $H$ , as the eruption rate increases, see Figure 2 (Mastin et al., 2009). The data of the ash plume height and the mass eruption rate compiled in Figure 2 is obtained by observations of the plume height and volume integration (Mastin et al., 2009). The height of the observed ash plumes is found by ground-based or airborne visual observations, radar measurements and cloud satellite temperatures (Mastin et al., 2009). The data for the erupted mass rate is obtained by volume integration over areas with deposition of ash particles and by multiplication with an average deposit density (Mastin et al., 2009). As seen in Figure 2, the uncertainty in eruption rate for a specific height is considerable and is in the order of a factor 10, making it difficult to accurately determine the eruption rate for a specific plume height.

Apart from the ash particles, a number of gases, e.g. water vapor, carbon dioxide ( $\text{CO}_2$ ), carbon monoxide (CO), sulfur dioxide ( $\text{SO}_2$ ), hydrogen fluoride (HF) and hydrogen sulfide ( $\text{H}_2\text{S}$ ) are produced in a volcanic eruption (Keller and DeVecchio, 2012; ATSDR, 2003). 90 % of all the gas that is emitted is water vapor and carbon dioxide (Keller and DeVecchio, 2012). Sulfur

dioxide emitted in an eruption have a smell resembling gunpowder and is of great danger to humans and animals, since it is a poisonous gas (Keller and DeVecchio, 2012). Sulfur dioxide can also react in the atmosphere to produce sulfate particles ( $\text{SO}_4^{2-}$ ) and acid rain and thereby cause acidification (Keller and DeVecchio, 2012). Hydrogen fluoride, which is emitted during a volcanic eruption, is an irritating gas and can in large concentrations lead to death for humans as well as for animals (ATSDR, 2003). Hydrogen fluoride causes irritation of the eyes, nose and skin and inhaling air with large concentrations can cause damage to the lungs and heart (ATSDR, 2003). Animals breathing air with hydrogen fluoride have shown damages to their lungs and testes (ATSDR, 2003). The largest problem for animals and livestock after a volcanic eruption is the intake of ash-covered grass and water (Runólfsson, 2010).

## **2.2 Grímsvötn and the eruption in 2011**

In the section below the traits of the studied volcano, Grímsvötn, will be highlighted as well as its eruption in 2011.

Grímsvötn is a stratovolcano located at the western part of the Vatnajökull icecap ( $64.42^\circ\text{N}$ ,  $17.33^\circ\text{W}$ ), meaning that it lies beneath several hundred meters of ice (Vatnajökull National Park, 2014). Through geophysical measurements in the 1990s it has been shown that Grímsvötn is roughly 15 km in diameter and has its highest peak at a height of over 1000 m above sea level (Vatnajökull National Park, 2014). Through history, Grímsvötn has been Iceland's most active volcano with at least 60 eruptions over the last 800 years (Vatnajökull National Park, 2014). A composite caldera, which is a large depression made during a severe eruption and the following collapse of the upper cone of the volcano, is located in the middle of the Icelandic volcano Grímsvötn (Vatnajökull National Park, 2014; Keller and DeVecchio, 2012). The composite caldera is made up of three parts, namely the north caldera ( $12 \text{ km}^2$ ), the south or also called the main caldera ( $20 \text{ km}^2$ ) and the east caldera ( $16\text{-}18 \text{ km}^2$ ) (Vatnajökull National Park, 2014). The majority of Grímsvötn's eruptions has taken place in the caldera (Vatnajökull National Park, 2014).

In May 2011 Grímsvötn had a subglacial, basaltic eruption which lasted for 7 days and the total volume of tephra erupted was  $0.6\text{-}0.8 \text{ km}^3$  (Stevenson et al., 2013). The bulk of tephra emitted during the eruption, was emitted during the first four days of the eruption. Measurements made on the sulphur concentration of the tephra points to that the eruption was produced by the formation of new magma from beneath (Sigmarsson, 2012). The eruption started at 19:00 UTC on the 21<sup>st</sup> of May and the initial ash plume reached a height of 15-20 km above sea level (Stevenson et al., 2013). This ash plume produced a 50-100 km wide umbrella cloud, which persisted until the 22 of May (Stevenson et al., 2013). From the 23<sup>rd</sup> of May, the eruption continued with a considerably less intensity and the plume height was less than 10 km above sea level until the end of the eruption on the 28<sup>th</sup> of May at 07:00 UTC (Petersen et al., 2012). The strength of the eruption decreased very rapidly and the height of the ash plume was 10 km or less already 24 h after the eruption started (Petersen et al., 2012).

Compared to the eruption of Eyjafjallajökull a year before, which had a maximum height of 8 km for the ash plume, the eruption of Grímsvötn was not expected to cause as much problems even though the total amount of ash particles was greater than for Eyjafjallajökull (Przyborski,

2011). This was due to the meteorological conditions and the fact that a large fraction of the ash particles were coarser resulting in a shorter airborne flight (Przyborski, 2011).

### **2.3 The Arctic and its characteristic atmospheric circulation**

In this section the mechanisms of the atmospheric circulation of the Arctic will be illuminated and discussed based on the effect on the dispersion of volcanic ash.

One elementary definition of the Arctic is that it is the region, or area, north of the Arctic Circle, i.e. 66.5 °N (Serreze and Barry, 2005). Mostly the Arctic consists of large areas of ocean surrounded by land masses (NSIDC, 2014c). A significant characteristic of this area is 24-hour daylight in summer and 24-hour darkness during winter. The number of days for these extreme conditions increases with latitude (Serreze and Barry, 2005). An additional definition of the Arctic is the area north of the arctic tree line, where the ground is frozen and dominated with shrubs and lichens (NSIDC, 2014c).

The atmospheric circulation in the Arctic is controlled by the strength of the high- and low-pressure centers in the region and the dominant centers are the Aleutian Low, Siberian High, Icelandic Low and Beaufort Sea High, which are called the “centers of action” in the atmospheric circulation of the Northern Hemisphere (NSIDC, 2014a). These weather patterns are all semi-permanent and their relative strengths can be compared and indices such as those describing the North Atlantic Oscillation and the Arctic Oscillation can be defined (NSIDC, 2014a).

The Aleutian Low is a semi-permanent low-pressure center located near the Aleutian Islands (Rodionov et al., 2007). The Aleutian Low is most intense during the winter, i.e. reaches its lowest pressure, and virtually disappears during the summer (Rodionov, 2007). It is important to underline that the Aleutian Low is a statistical feature and an average of several synoptic maps that represent the location where the cyclones most often reach their maximum over a specific period (Rodionov, 2007).

The semi-permanent low-pressure center situated close to Iceland, typically between Iceland and southern Greenland, is called the Icelandic Low (NSIDC, 2014b). The Icelandic Low has its maximum during winter and in summer it weakens and splits into two systems; one located near Davis Strait and one west of Iceland (NSIDC, 2014b).

The Siberian High is an intense and cold anticyclone (high-pressure center) situated over eastern Siberia in winter time, and the Beaufort Sea High also dominant in winter time, is a high-pressure center located over the Beaufort Sea (NSIDC, 2014b).

Apart from the high- and low-pressure centres, the polar jet stream affects the dispersion patterns of airborne particles in the Arctic. A jet stream is a relatively small and narrow band in the atmosphere where the wind is strong (Ahrens, 2013). The jet stream is located in the tropopause gaps, where the air between the troposphere and stratosphere is interchanged (Ahrens, 2013). The jet stream positioned in the northern latitudes is called the polar jet stream and is situated at a height of approximately 10 km (Ahrens, 2013). The typical meridional pattern of the polar jet stream is of great importance for the heat transport of the Earth (Ahrens, 2013). In the Northern Hemisphere, the air moving south brings cold air with it and the air

flowing northward, brings warm air, maintaining the overall heat budget (Ahrens, 2013). The formation of the jet stream is a result of an imbalance in energy between the high and low latitudes.

The polar jet stream is closely connected to the polar front, which separates the cold polar air and the more temperate mid-latitude air. This rapid change in temperature over a small distance causes a rapid change in pressure and this sharp change in pressure along the front is the origin of the steep pressure gradient that intensifies the wind speed and gives rise to the jet stream (Ahrens, 2013). The temperature contrast is strongest in winter and weakest in summer, thereby causing seasonal variations in the strength and location of the polar jet stream. In winter time the polar jet stream is stronger and extends further south due to colder temperatures in the northern latitudes (Ahrens, 2013). In summer, the jet stream is weaker and is found at higher latitudes (Ahrens, 2013).

The Arctic front is a transition between two air masses with different characteristics in the Arctic (Ahrens, 2013). The front separates cold air from extremely cold arctic air and it has a very low vertical extension of one or two kilometres compared to several kilometres for most mid-latitude fronts (Ahrens, 2013). The Arctic front also has a seasonal variation in extension, which affects the dispersion of volcanic ash during a volcanic eruption (Ahrens, 2013).

#### 2.4 Transport of particulates to the Arctic

In the following paragraph the mechanisms and importance of the polar dome for the dispersion of gases and particles will be explained. The transport of ash particles to the Arctic is dependent on several factors, such as winds, location of emission sources etc. (Quinn, 2011). The Arctic region can be described by surfaces of constant potential temperature that creates shells over the Arctic and generates a polar dome (Klonecki et al., 2003; Stohl, 2006), as seen in Figure 3.

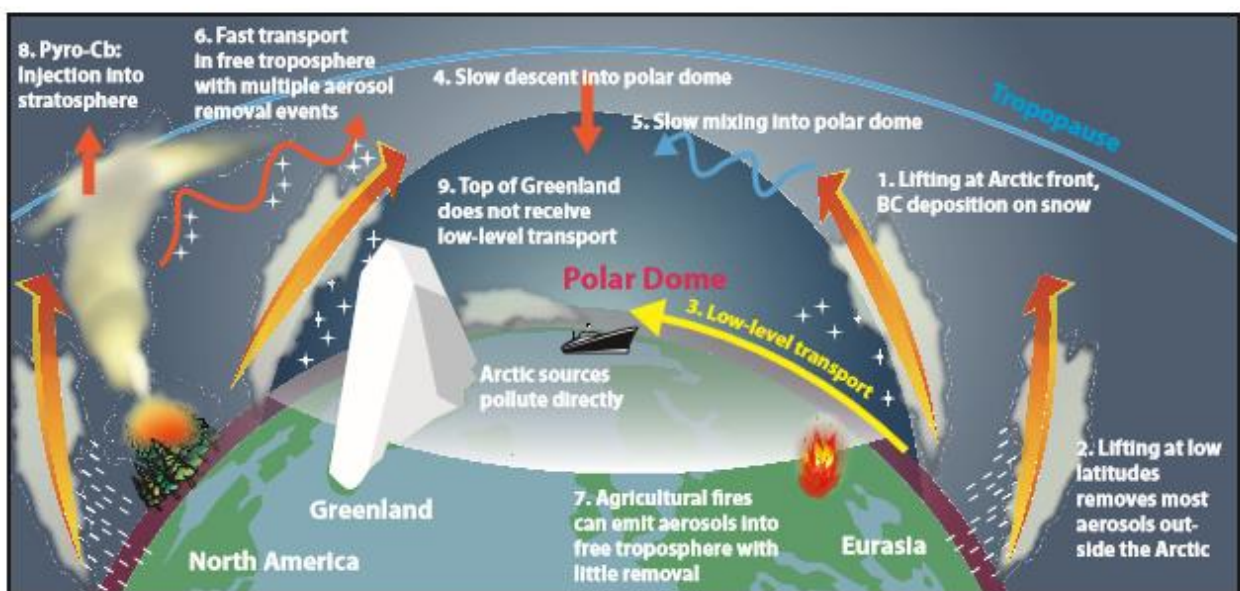


**Figure 3.** A schematic figure displaying the Arctic polar dome (Quinn, 2011). The picture is intended for black carbon, however, the transport pathways for volcanic ash is almost analogous. Volcanic ash particles are, however, emitted at a greater height and have different deposition characteristics compared to black carbon making some pathways more relevant for ash particles, e.g. pathway 1.

Typical weather conditions, especially in wintertime, in the Arctic is a smooth snow-covered surface, with low temperatures and low solar insolation (Guenther and Lamb, 1989). These conditions affect the atmospheric boundary layer (ABL), which is highly dependent on the thermal stability and the roughness of the surface (Guenther and Lamb, 1989). The result of these parameters is a strong surface inversion which leads to an exceptionally high static stability of the Arctic air mass located inside the dome (Quinn, 2011). The high static stability causes low turbulence intensities and hinders the vertical exchange among the boundary layer and the free troposphere and thereby the deposition of particles (Strunin et al., 1997). The southerly part of the Arctic lower troposphere is inaccessible from the rest of the atmosphere by the Arctic front, i.e. a transportation barrier for the Arctic (Barrie, 1986). Since potential temperatures are almost preserved on a short time scale, particles emitted into an air mass south of the polar dome must rise above the dome and follow the isentropes and enter the Arctic by the middle or upper troposphere above the dome, i.e. passageways 1 and 2 in Figure 3 (Carlson, 1981; Iversen, 1984; Barrie, 1986). Volcanic ash particles are always emitted into a warm air mass making an ascent above the polar dome a probable pathway for dispersion into the Arctic.

The paths of transportation to the Arctic vary from season to season (Quinn, 2011). During winter, the Arctic front extends further south compared to its summer extension, particularly over Eurasia, making the appearance of the polar dome different from its summer appearance (Barrie, 1986; Heidam et al., 2004).

During winter and spring, the lower tropospheric circulation in the polar region is characterised by high pressure over the continents and low pressure over the northern parts of the Pacific and Atlantic Ocean (Nuttall and Callaghan, 2000). The locations of the pressure systems result in an Arctic front that is further south during winter compared to summer (Nuttall and Callaghan, 2000). Typically, the strong Siberian high-pressure system forces air along its west side and further north into the Arctic (Nuttall and Callaghan, 2000). The high-pressure ridge that often is located over North America pushes the air south out of the Arctic (Nuttall and Callaghan, 2000). The characteristic flow in the Arctic in wintertime is therefore out of Eurasia and into the Arctic and out of the Arctic and into North America (Nuttall and Callaghan, 2000). The time span for atmospheric transport from Europe to Alaska in the Arctic during winter is approximately 13-16 days, but in summer time this northward transport decreases making the time span significantly longer (Nuttall and Callaghan, 2000). The residence time for particles in the Arctic atmosphere during winter is up to 20-30 days, compared to 2-5 days in summer due to increased precipitation (Nuttall and Callaghan, 2000).

## **2.5 Environmental and human effects of volcanic eruptions**

The impact of volcanic eruptions on the environment and humans, as well as animals, can be significant as will be explained in the following section. The environmental and human effects of a volcanic eruption are dependent on the magnitude of the eruption, the intensity (the rate at which emissions are ejected into the atmosphere; which also controls the plume height), where the volcano is located, the properties of the emitted particulates and gases (both physical and chemical) and their residence time in the atmosphere (mainly dependent on the eruption intensity and the primary particle-size distribution) (Durant et al., 2010). Apart from the effect on humans and animals the volcanic particulates affect the energy budget of the atmosphere by

scattering and absorption of solar and terrestrial radiation (Durant et al., 2010). Long-term climatic effects due to volcanic eruptions are caused by volcanogenic stratospheric sulphate aerosols (SSA) (Durant et al., 2010). Compared to the SSA the tropospheric volcanic aerosols are much more short-lived and are more rapidly transported to the surface by wet deposition (Durant et al., 2010). If the ash particles and the SO<sub>2</sub> reach the stratosphere the climatic effect is on the scale of months to years, however in the troposphere the eruption products are sedimented and precipitated out relatively quickly (Niemeier, 2009). However, extensive emission of volcanogenic particulates to the troposphere can nevertheless be the cause of changing effects in the local and regional environment (Durant et al., 2010).

The gaseous SO<sub>2</sub> emitted in a volcanic eruption reacts by photooxidation in the atmosphere producing numerous sulphuric acid (H<sub>2</sub>SO<sub>4</sub>) aerosol particles with a diameter of <0.02 µm in the stratosphere (Durant et al., 2010). The sulphuric acid aerosol particles grow by coagulation to larger sizes (Durant et al., 2010). Nearly all the sulphuric acid produced nucleates on pre-existent condensation nuclei, creating liquid sulphuric acid- and water-particles, which is the origin of SSA (Durant et al., 2010). Volcanogenic stratospheric sulphate aerosols scatter shortwave radiation back to space, which gives a higher planetary albedo, and absorb long-wave terrestrial radiation (Durant et al., 2010).

Fallout of tephra and condensation of volcanic gases in the troposphere during a volcanic eruption result in numerous condensation nuclei, which increase cloud formation and thereby cause a higher albedo and local surface cooling (Sigurdsson, 1990).

The volcanic ash produced in an eruption can function as a nutrient to the oceans (Durant et al., 2010). According to Duggen et al. (2009) the addition of bio-accessible iron from the ash particles to the oceans can cause severe phytoplankton blooms and affect nitrogen fixation if the addition takes place in a productive but iron-poor ocean. If the supply of ash particles is continuous for months, or even years, and the iron concentration is sufficient there might be a chance of CO<sub>2</sub> removal by the stimulated biological activity (Durant et al., 2010).

## **2.6 Aviation and safety concentrations for ash particles**

Apart from environmental and human effects, volcanic ash also affect air traffic. The following section displays the current restrictions for levels of ash particles in the atmosphere.

After the large volcanic eruption of Eyjafjallajökull in 2010, that caused large disruptions in the air traffic, measures have been taken in case a similar incident occurs in the future (CAA, 2014). In UK airspace and in nearly all of Europe the same regulations apply when ash particles are present in the air (CAA, 2014). The airspace is divided into certain regions based upon the amount of ash particles present in the air and the amount of ash particles is evaluated by the Met Office's Volcanic Ash Advisory Centre (CAA, 2014). The air space is divided into three categories based upon the density of ash particles present in the air (CAA, 2014). The three categories are low, medium and high density (CAA, 2014). Low density corresponds to air space where ash particles have a concentration equal to or less than 2 milligrams per cubic metre of air, medium density corresponds to concentrations larger than 2 but smaller than 4 milligrams per cubic metre and high density represents concentrations equal to or larger than

4 milligrams per cubic metre (CAA, 2014). As the uncertainty in eruption rate for a volcano is on the order of 10 it can be argued that the medium category is of no relevance, since it is very difficult to accurately claim that ash concentrations fall into that category. Therefore, is this “grey-zone” mainly helpful for the economy of the aviation corporations who are able to fly in conditions with more ash particles present in the air compared to previous restriction values.

## **2.7 The effect of ash particles on snow and ice albedo**

The change of snow and ice albedo is of great importance for the climate and in the following section the effect of ash particles on snow and ice albedo will be explained.

Typical values for the albedo of snow and ice are in the range of 0.2 to 0.85, and the amount of absorbed shortwave radiation therefore varies considerably (Cuffey and Paterson, 2010). The albedo of snow decreases as the concentration of particulate matter increases at the snow-covered surface (Higuchi and Nagoshi, 1977; Warren and Wiscombe, 1980; Woo and Dubreuil, 1985). Particles deposited on a snow-covered surface normally affect the albedo of the surface until the particles are buried by snowfall and no longer have an effect on the surface’s albedo (Conway et al., 1996). During conditions of melt the particulate matter can be transported to a larger depth or away from the snow-covered surface and thereby no longer have any effect on the albedo (Conway et al., 1996). The mobility of particulate matter is not well-known. However many particles are assumed to have a low mobility (Conway et al., 1996).

The effect of ash particles on snow albedo, shown in Table 1 and Figure 4, displays the difference in albedo change between different amounts of ash particles and residence times on a snow-covered surface (Conway et al., 1996). A1 and A2 represent the same amount of ash particles (Conway et al., 1996). However the residence time for the ash particles is 12 days longer for A2 (214 days) compared to A1 (202 days) (Conway et al., 1996). The reduction of snow albedo, as a result of deposition of ash particles, is nearly 30 % compared to natural snow for A1 and A2 (Conway et al., 1996). The reduction for A1 and A2 is comparable, demonstrating that ash particles have a long-term effect on snow albedo (Conway et al., 1996). Increasing the amount of ash particles by a factor of 4, shown by Figure 4 as A3, illustrates a reduction of the snow albedo of 50 % compared to natural snow (Conway et al., 1996).



**Table 1.** Amount and days of application of volcanic ash particles on a snow-covered surface (Conway et al., 1996).

	Contaminant	Amount, kg m <sup>-2</sup>	Day of Application
	natural snow	...	...
A1	volcanic ash	0.0167	202
A2	volcanic ash	0.0167	214
A3	volcanic ash	0.0668	214
L1	hydrophobic soot	0.0033	202
L2	hydrophobic soot	0.0033	214
L3	hydrophobic soot	0.0330	214
H1	hydrophylic soot	0.0033	202

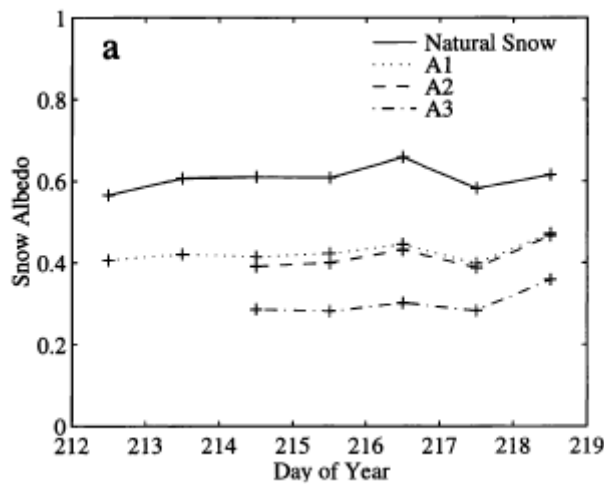


**Figure 4.** The effect of quantity and residence time of ash particles on snow albedo (Conway et al., 1996). A1 corresponds to a deposition of 16.7 g/m<sup>2</sup> and an application time of 202 days. The A2 curve corresponds to the same amount of ash particles as A1, but an application time of 214 days. For the A3 curve the amount of ash particles has increased to 66.8 g/m<sup>2</sup> and the application time is 214 days.

Apart from affecting the albedo by direct deposition of volcanic ash over vast areas, the volcanic ash can be collected in small holes on top of glaciers, cryoconite holes, and affect the albedo by biological processes (Bøggild et al., 2010). Cryoconite holes are water-filled depressions and the typical size of cryoconite holes are diameters of < 1 m and depths of < 0.5 m, see Figure 5 (Bøggild et al., 2010). The cryoconite holes form when the inorganic and organic debris melts into the ice with the help of solar heating (Bøggild et al., 2010). The cryoconite holes are habitation for viruses, bacteria and algae (Bøggild et al., 2010). These microbial communities add dark biomass and pigments to the ice and can absorb nutrients, such as nitrates, from the atmosphere; thereby survive the harsh, cold conditions on top of glaciers (Bøggild et al., 2010; Cook and Box, 2014).

The albedo of an ice surface covered by a uniform debris cover, either a light, intermediate or dark cover, is much lower compared to an ice surface covered by cryoconite holes, despite the fact that cryoconite holes contain a larger volume of debris (Anesio, 2009). The increase of albedo of a surface covered with cryoconite holes is a result of the concealment of the debris and the sunlight is therefore required to interact with the clean, white ice above the holes (Anesio, 2009). If the debris on the ice surface clumps together to form clusters its absorptive capability is lowered, since the lowering of the albedo by debris is largest when it is uniformly distributed (Anesio, 2009). The albedo for ice covered by uniformly distributed debris is 0.2-0.4, while the albedo for ice with cryoconite holes is 0.6 despite the larger amount of debris (Anesio, 2009). Thus, the secondary biological effect is greater than the direct deposition of ash fall.

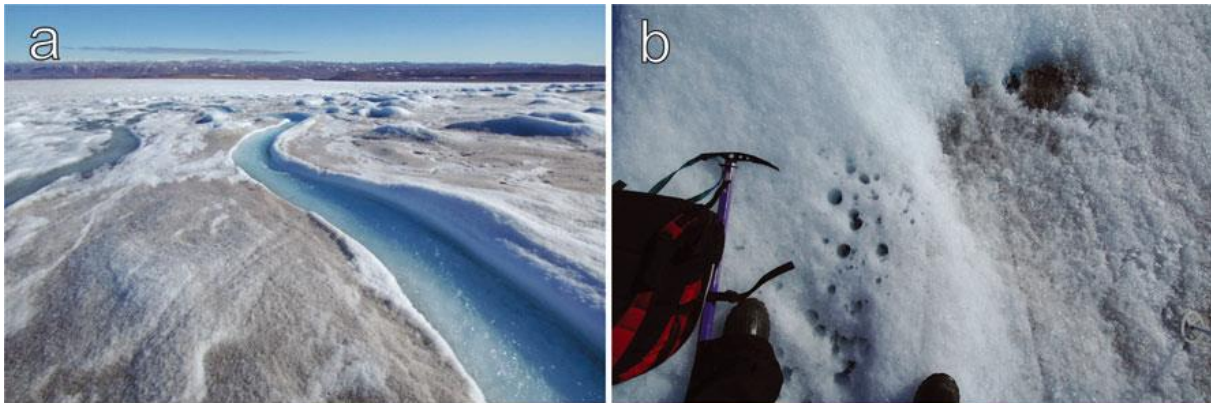


**Figure 5.** The appearance of a uniform debris cover compared to cryoconite holes on an ice surface (Bøggild et al., 2010). (a) A uniform debris cover without cryoconite holes. (b) Cryoconite holes on the left compared to a uniform debris cover on the right.

### 3. Method

To evaluate and determine the dispersion and deposition of volcanic ash from the 2011 eruption scenario of Grímsvötn both scientific reports and computer programmes, modelling the dispersion and deposition of volcanic ash, have been used. The literature and scientific reports used in this report is found by the use of the database “LibHub” at the University of Lund. The literature is carefully examined and evaluated for coherency to the project and its aim. The model used to describe the dispersion and deposition is the Danish Emergency Response Model of the Atmosphere (DERMA), which produces a series of figures describing the dispersion and deposition. To be able to interpret the results the programme MetGraf, used at DMI, is utilized.

#### 3.1 Dispersion modelling

To simulate the long-range atmospheric dispersion of volcanic ash from the 2011 eruption of Grímsvötn to the Arctic, a model called Danish Emergency Response Model of the Atmosphere (DERMA) is used. The DERMA model is a three-dimensional Lagrangian stochastic puff-particle model (Sørensen et al., 2011). All released particles from the 2011 eruption of Grímsvötn that are studied, in this case ash particles between 0-60  $\mu\text{m}$  in diameter, are advected by the three-dimensional wind (Sørensen et al., 2007). All particles are surrounded by a concentration field called a puff, and the total sum of these puffs represents the ash plume in the DERMA model (Sørensen et al., 2007).

DERMA is capable of describing the atmospheric dispersion, deposition (both wet and dry) and diffusion of volcanic ash originating from a volcanic eruption and evaluate these parameters for specific meteorological conditions (Sørensen et al., 2007). The scale for which the model can predict the dispersion, deposition and diffusion of the ash plume is from 20 km to a global scale (Sørensen, 2007). Apart from modelling the dispersion of ash particles, the model is also used to describe the dispersion of airborne spread of animal diseases, e.g. foot-and-mouth disease, chemical and radioactive substances and biological warfare agents (Sørensen, 2007).

The input needed for the DERMA model is the height of the ash column above the volcano and the reduction factor describing the fraction of small particles with the ability to travel long distances with the winds (Sørensen, 2014). With the help of the height of the ash column the model is able to predict the eruption rate according to the best fit in Figure 2 by Mastin et al. (2009) (Sørensen, 2014). The input of the reduction factor makes it possible to observe a specific size range of particles, in this case 0-60  $\mu\text{m}$ . The value of the reduction factor was 1 % in the beginning of the 2011 Grímsvötn eruption, meaning that 1 % of the total erupted mass is in the size interval of 0-60  $\mu\text{m}$ . With time the reduction factor increased to 5 %, as the amount of emitted mass decreased. The model does not describe the deposition close to the volcano, which is dominated by coarser volcanic ash particles, as they are omitted from the dispersion calculations in DERMA.

The validation of the model has been verified many times against measured data representing the unintentional or planned release of traceable substances (Sørensen, 2007). However, when studying the release of volcanic ash there are sources of errors that will affect the modelled dispersion of ash. For example, the initial ash column is assumed to have the shape of a vertical

line upwards into the air above the summit, and the concentration of ash is assumed continuous and constant with height inside the column (Sørensen, 2014). This assumption of an initial line-shaped ash column and continuous concentration is the simplest way to model the dispersion situation during a volcanic eruption and as a result of its simplicity it does not describe the pulsating eruption in detail (Sørensen, 2014). The height of the ash plume is not a fixed height at a specific time, since the volcano emits the ash particles in pulses (Sørensen, 2014). Therefore the height of the ash plume and the modelled dispersion are to some extent inaccurate. Most of the uncertainties lies with the source, in this case the volcano itself. For example, the eruption rate is assessed by the best fit estimation made by Mastin et al. (2009) in which there is a great uncertainty. The reduction factor is also a source of error as it is based on sampling of ash particles at ground-level, making it impossible to review all types of particulate matter from a volcanic eruption (Sørensen, 2014). Yet another potential uncertainty is the parameterization of the turbulent diffusion of ash out of the ash plume (Sørensen, 2014).

The area of importance is the Arctic and the ash release scenario used corresponds to the eruption of Grímsvötn in 2011. The instantaneous concentration for five vertical levels (2 m, 2 km, 5 km, 10 km and 15 km) and the total deposition on the surface is evaluated for a period of 14 days. The period of 14 days is chosen to give the particles a sufficient time frame to be able to reach the Arctic and the five vertical levels are chosen to display the surface, the jet stream, the atmospheric boundary conditions and the cruising height for air traffic.

### **3.2 Meteorological data**

The DERMA model uses meteorological data from the Numerical Weather Prediction (NWP) model HIRLAM (High Resolution Limited Area Model) (HIRLAM-T15) in operation at the Danish Meteorological Institute (DMI) (Sørensen et al., 2007).

The NWP model, HIRLAM, is available in different versions which all cover slightly different geographical areas (Hansen, 2014). Three of the most important versions of the model and their respective geographical area are displayed in Figure 6. The weather model makes predictions on the development of the weather by the use of the supercomputer at DMI (Hansen, 2014). The use of the supercomputer is necessary due to the complexity of the atmosphere and its physical processes that need to be considered in a large number of points to describe the weather satisfactory (Hansen, 2014). The calculations and predictions about the weather is made for 40 vertical levels up through the atmosphere (see Figure A1) and the number of horizontal points is a significantly larger number due to the relatively large geographical area (Hansen, 2014).

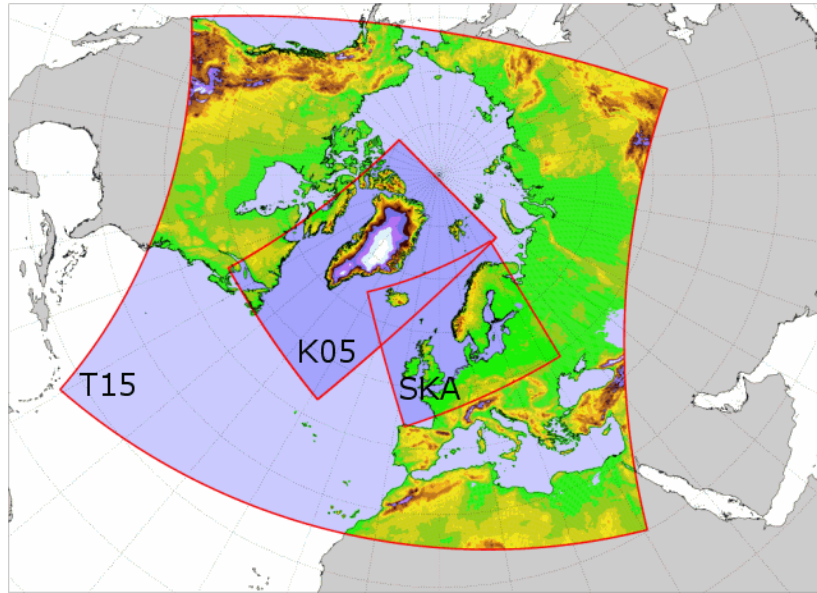


**Figure 6.** The geographical area in the Northern Hemisphere covered by the HIRLAM T15 model (Hansen, 2014). The different colours indicate the topography in the various areas.

Before the model is run the initial weather state needs to be known with as good precision as possible and this is done by the use of measurements from e.g. weather balloons and satellites (Hansen, 2014). The most important meteorological parameters evaluated by the weather model is the temperature, the wind, the precipitation and cloud cover (Hansen, 2014). In Table 2 is some of the features of the HIRLAM T15 model specified (Hansen, 2014).

**Table 2.** Characteristics of the HIRLAM T15 model (Hansen, 2014).

HIRLAM T15	
Number of vertical levels	40
Horizontal resolution	0.15° (16 km)
Time step	400 s
Model for the boundary values	ECMWF
Length of forecast	60 h

All available meteorological data from HIRLAM, e.g. cloud cover, wind, humidity, precipitation, temperature, pressure, corresponding to the chosen cases are retrieved from the meteorological archive at DMI and used in the model DERMA to give results regarding the atmospheric transport and deposition of volcanic ash. The studied time periods are chosen based upon the location of the Arctic front and the size of the polar vortex. The winter case is chosen so that the Arctic front has a more southerly position and a large polar vortex, while the summer case has a small polar vortex and an Arctic front with a more northerly position. By the observation of pressure maps displaying different months in different years the month January was chosen for the winter scenario, since the month fulfilled the criteria of a large polar vortex and a southerly position of the Arctic front. The month chosen for the summer scenario was August, due to the small extent of the polar vortex and the high latitude position of the Arctic front. So the chosen winter scenario is the 8<sup>th</sup> of January 2014 to the 22<sup>nd</sup> of January 2014 and the chosen summer scenario is the 10<sup>th</sup> of August 2006 to the 24<sup>th</sup> of August 2014.

The meteorological conditions, such as the wind and precipitation, during the two time periods are studied by the use of MetGraf. MetGraf is a programme that illustrates several meteorological parameters, such as the wind and precipitation, by the use of an archive of meteorological data at DMI (Sørensen, 2014). The data from MetGraf is used to interpret and discuss the results. When retrieving data concerning the wind patterns the different heights are given in vertical levels, with a total number of 40 levels (Korsholm, 2014). Each level corresponds to a pressure level, which also corresponds to a certain height. To determine the corresponding vertical level to a certain height, a standard atmosphere is used (Korsholm, 2014).

#### 4. Result and discussion

The height of the ash plume and the eruption rate for the 2011 eruption of Grímsvötn is displayed in Figure 7 and 8 respectively. The tendency is an increase of the mass eruption rate as the height of the ash plume increases, as expected from Figure 2.

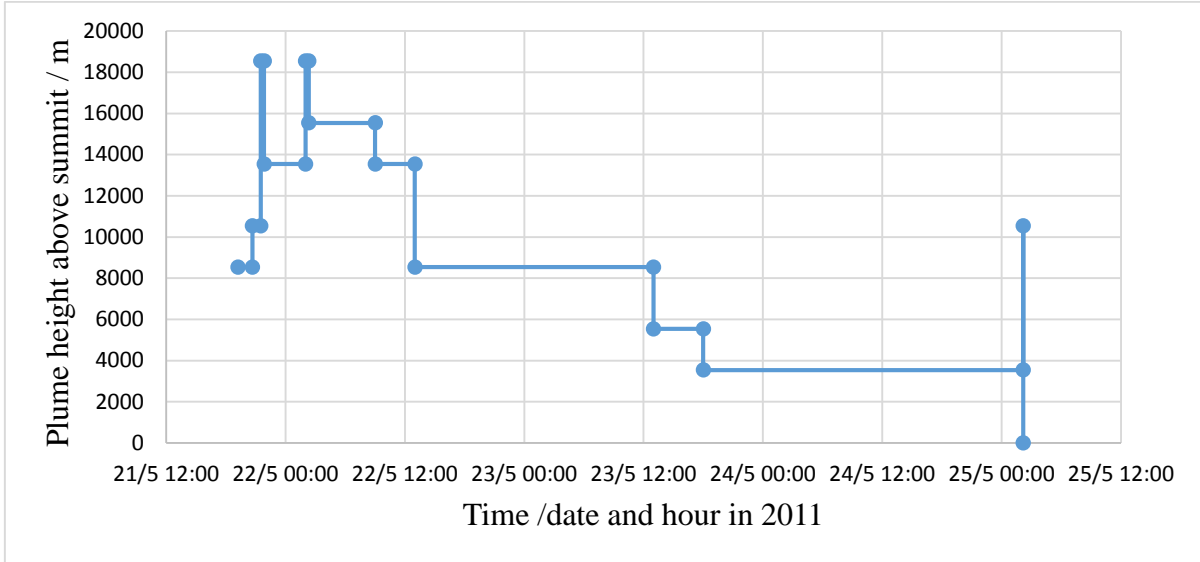


**Figure 7.** The variation in height of the ash plume after the start of the 2011 Grímsvötn eruption. The data used is obtained from UK Met Office (2011).

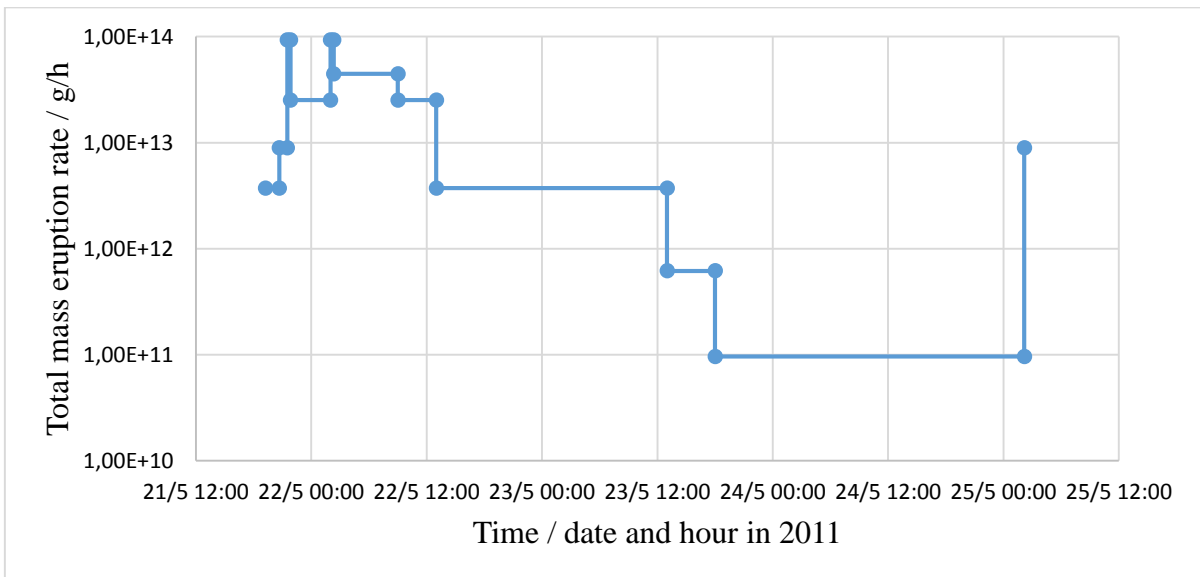


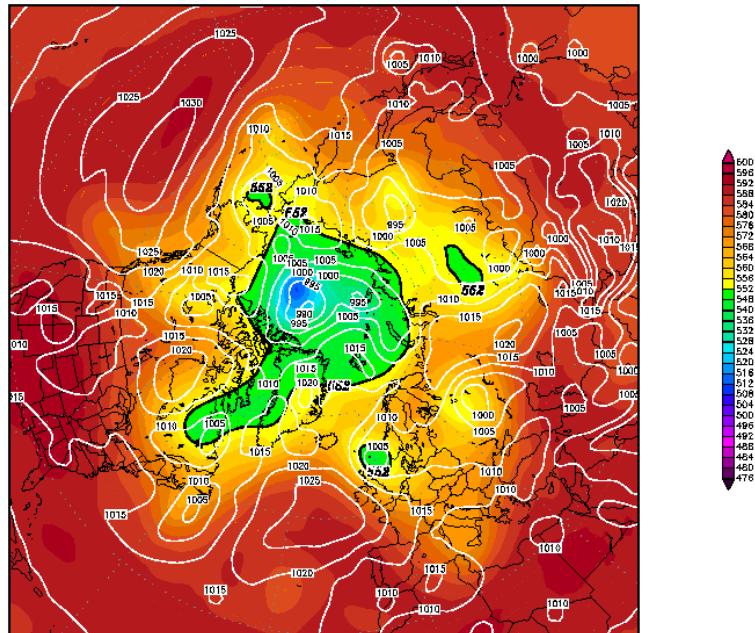
**Figure 8.** The variation of total mass eruption rate with time for the 2011 Grímsvötn eruption. The data used is obtained from UK Met Office (2011).

As DERMA produces a large number of graphs demonstrating the dispersion and deposition of volcanic ash from the 2011 eruption of Grímsvötn to the Arctic, only a few representative graphs are presented in the report. In the following two sections the characteristics of the summer and winter period regarding the sea level pressure, precipitation, wind pattern, dispersion and deposition of volcanic ash will be presented and the differences between the seasons will be illustrated.

#### 4.1 The 2006 summer scenario

The sea level pressure pattern representing the summer scenario in 2006 is dominated by a high-pressure centre located southwest of Iceland, which moves south and is replaced by a low-pressure centre at the end of the studied period, as can be seen in Figure 9, 10 and 11. As a whole, the period is dominated by multiple high-pressure centres. The arctic front is positioned at high latitudes and the polar dome has a small extension, displayed in Figure 9, 10 and 11, as can be seen by the differences in geopotential height.

Init : Thu,10AUG2006 00Z Valid: Thu,10AUG2006 00Z  
 500 hPa Geopot. (gpm) und Bodendruck (hPa)

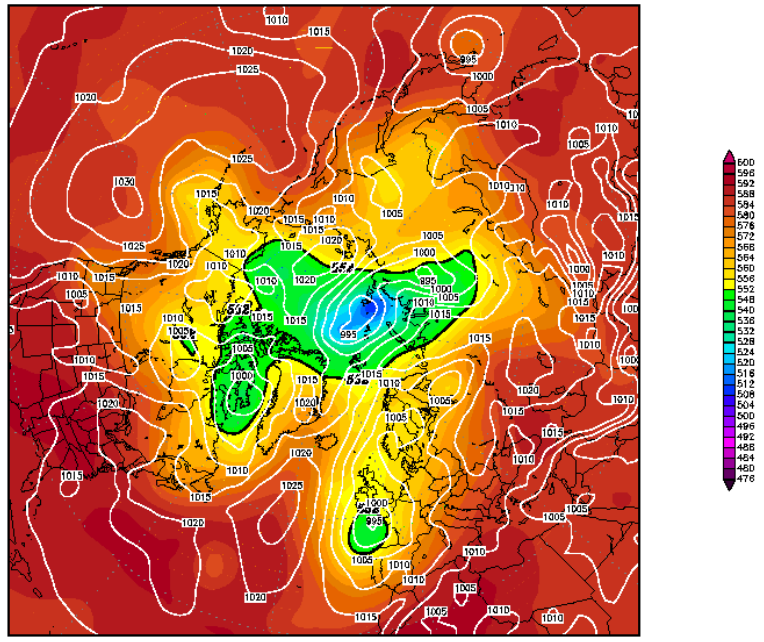


Daten: GFS-Modell des amerikanischen Wetterdienstes  
 (C) Wetterzentrale  
 www.wetterzentrale.de

**Figure 9.** The mean sea level pressure in the Arctic on the 10<sup>th</sup> of August 2006 valid at 00 UTC (Wetterzentrale, 2014).



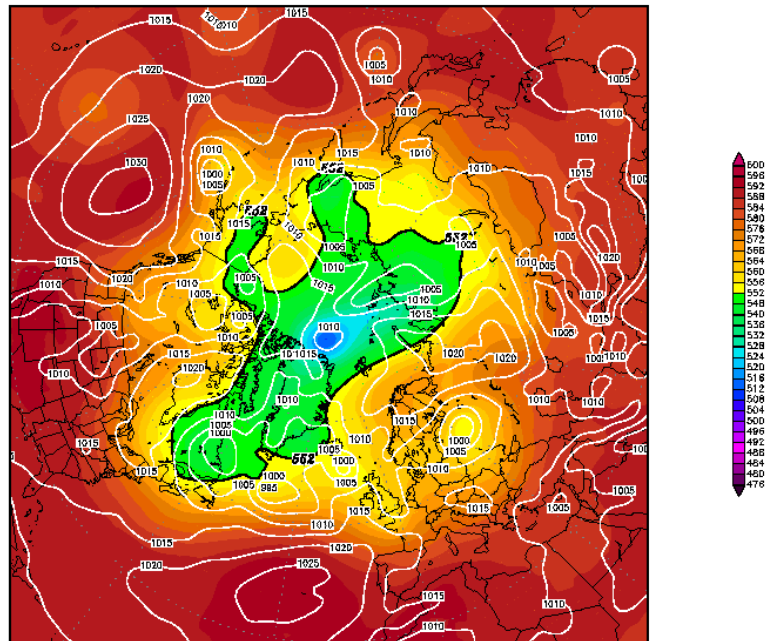
Init : Thu,17AUG2006 00Z Valid: Thu,17AUG2006 00Z  
500 hPa Geopot. (gpm) und Bodendruck (hPa)



Daten: GFS-Modell des amerikanischen Wetterdienstes  
(C) Wetterzentrale  
www.wetterzentrale.de

Figure 10. The mean sea level pressure on the 17<sup>th</sup> of August 2014 valid at 00 UTC (Wetterzentrale, 2014).

Init : Thu,24AUG2006 00Z Valid: Thu,24AUG2006 00Z  
500 hPa Geopot. (gpm) und Bodendruck (hPa)



Daten: GFS-Modell des amerikanischen Wetterdienstes  
(C) Wetterzentrale  
www.wetterzentrale.de

Figure 11. The mean sea level pressure on the 24<sup>th</sup> of August 2014 valid at 00 UTC (Wetterzentrale, 2014).

The images produced with the help of DERMA and the input data displays the instantaneous concentration of volcanic ash at the chosen heights. The dispersion of ash at 2 m, displayed in Figure A2:1, illustrates that the main part of the ash particles are dispersed and suspended over Europe and the Mediterranean. The concentration of ash particles is low and reaches  $0.001 \text{ g/m}^3$  as a maximum. The first days after the eruption show no or small concentrations of ash at the 2 m level, however thereafter the concentration of ash particles increases due to downward mixing. The dispersion over the Arctic at 2 m is almost completely absent in the summer period of 2006.

At a height of 2 km the dispersion of ash has the appearance displayed in Figure A2:2. The initial plume moves towards the south in over Europe and as the dispersion continues the ash particles become more evenly distributed in the Northern Hemisphere and covers a larger geographical area, as seen on the right in Figure A2:2.

At a height of 5 km the majority of the ash particles moves towards Europe and the Mediterranean, as seen in Figure A2:3. The instantaneous concentration is largest, approximately  $0.001 \text{ g/m}^3$ , at the beginning of the eruption and becomes more uniform as the eruption progress.

The ash dispersion at a height of 10 km is dominated by dispersion mainly outside the Arctic and the concentration reaches a maximum at the beginning of the 2006 period and becomes more uniform with time, seen in Figure 12. The maximum of the instantaneous concentration during the period is  $0.01 \text{ g/m}^3$ .

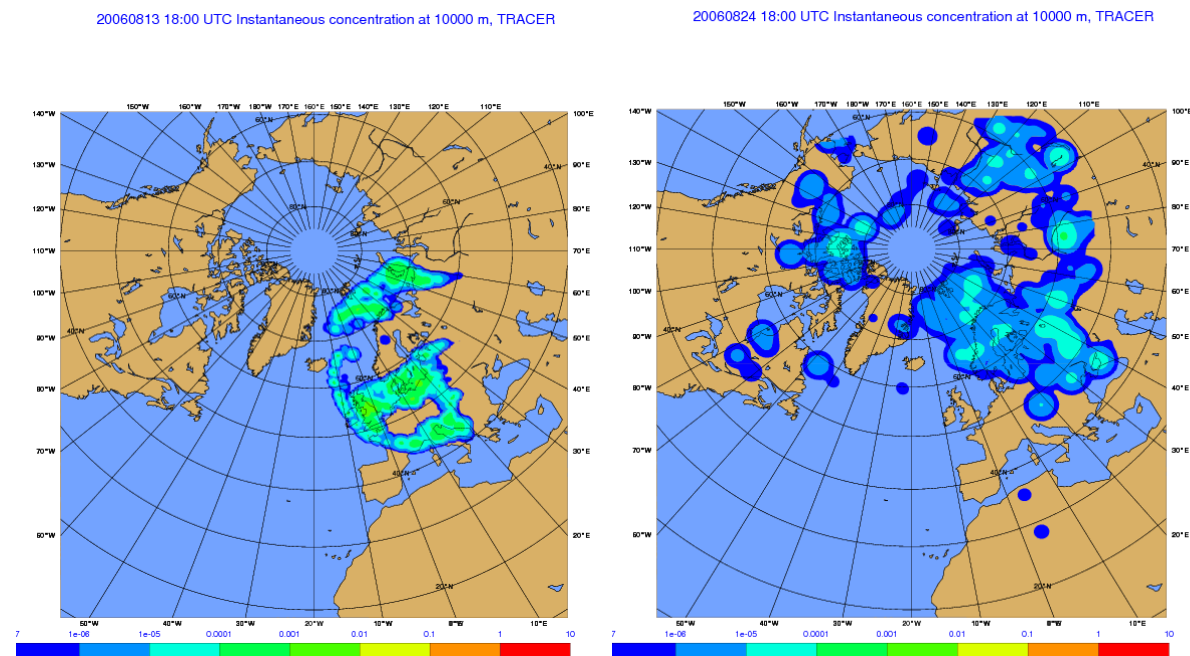


**Figure 12.** The instantaneous concentration of ash in  $\text{g/m}^3$  at 10 km above the surface at 18 UTC on the 13<sup>th</sup> and 24<sup>th</sup> of August 2006, calculated by DERMA.

As seen in Figure A2:4, the dispersion and concentration at 15 km is very low and the main part of the volcanic ash remains outside the Arctic. The low concentration of ash at an altitude of 15 km is due to the height of the eruption plume, which reaches a height of 15 km for only brief time periods during the eruption.

The location of the polar jet stream and its typical meandering appearance is depicted in Figure 13. The wind velocity in the jet stream is high and the white colour indicates that the velocity is higher than the attached scale. It can also be seen that the wind direction in the polar jet stream around Iceland is northerly, making the dispersion of volcanic ash at a height of 10 km mainly southerly.

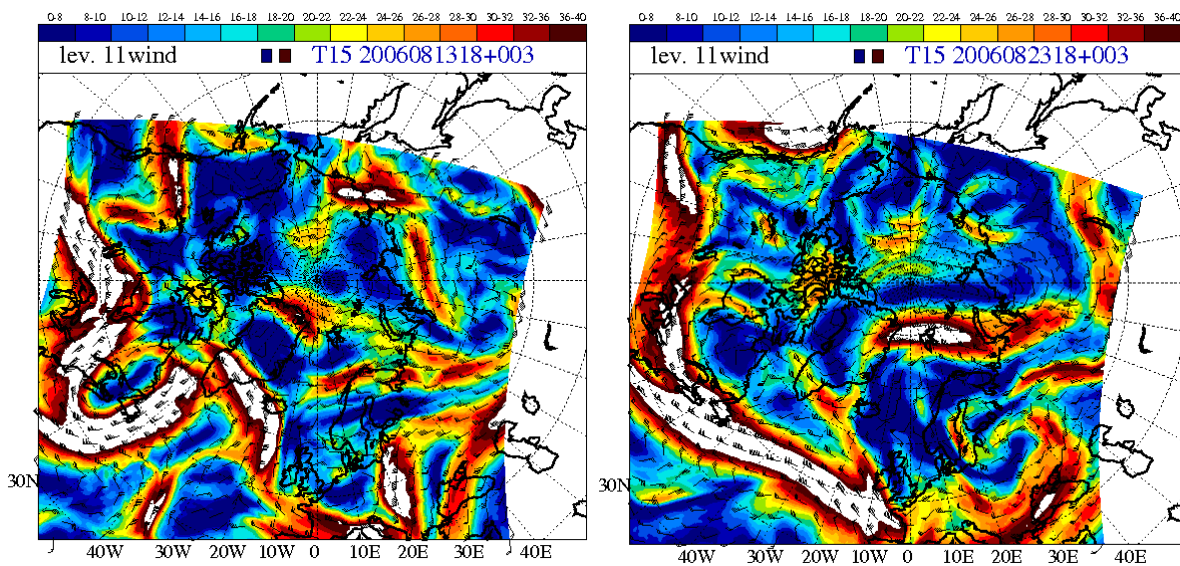


**Figure 13.** The polar jet stream and its position in the Northern Hemisphere for the 13<sup>th</sup> and 23<sup>rd</sup> of August 2006 valid at 21 UTC (MetGraf, 2014). The jet stream is located at a height of approximately 10 km and its strength is beyond the attached scale, as indicated by the white colour.

The 5-hour accumulated precipitation in the Arctic in Figure 14 is low and the demonstrated situation is representative for the entire studied period, which receives little precipitation. The overall precipitation in the entire Northern Hemisphere is low.

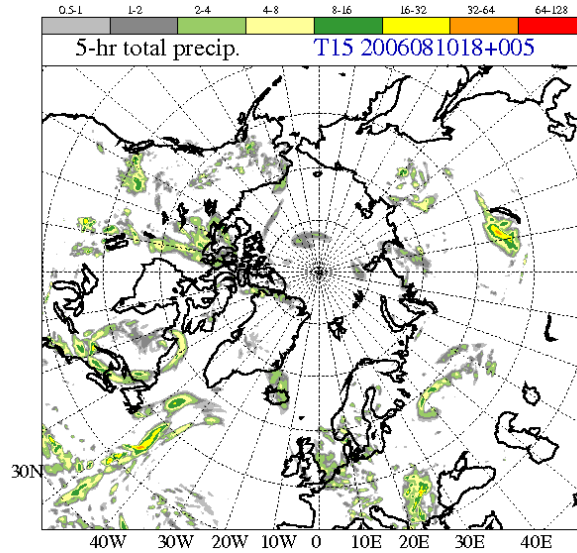


**Figure 14.** The 5-hour accumulated precipitation for the 10<sup>th</sup> of August 2006 valid at 23 UTC (MetGraf, 2014).

The total deposition of ash particles for the two week period, calculated and displayed by the help of DERMA, is presented in Figure 15 and the largest deposition is received in Europe and the Mediterranean. The Arctic merely receives small amounts of ash particles at the Earth's surface. The total deposition is at a maximum of 1 g/m<sup>2</sup> in Europe and the Mediterranean (see Figure 15).

20060824 18:00 UTC Total deposition at 0 m, TRACER

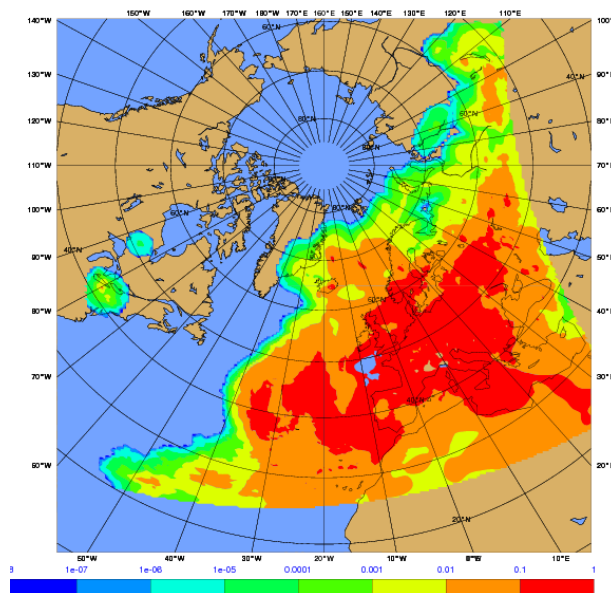
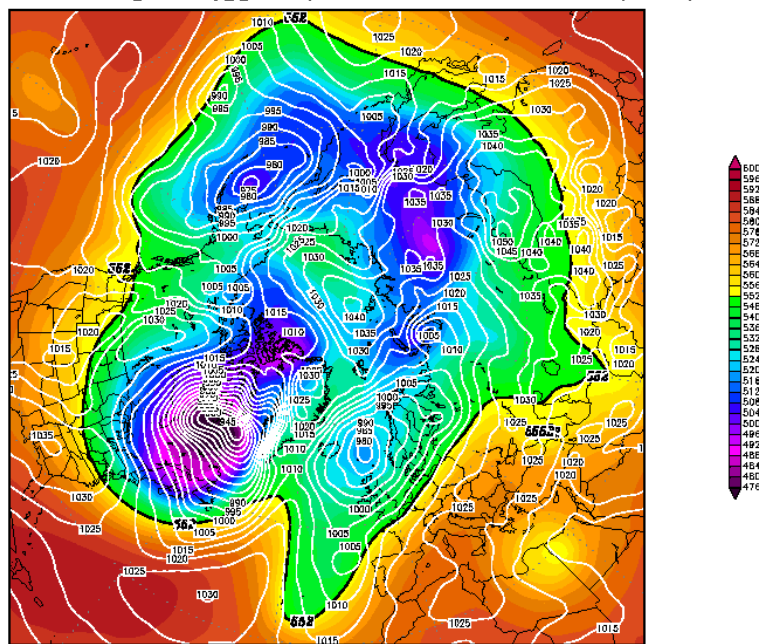


**Figure 15.** The calculated result of DERMA for the total deposition of ash particles in g/m<sup>2</sup> for the summer scenario in 2006.

#### 4.2 The 2014 winter scenario

The sea level pressure pattern representing the winter scenario around Iceland in 2014 is dominated by two low-pressure centres, one to the west of Iceland and one to the east, as seen in Figure 16. The Arctic as a whole is dominated by a number of different low-pressure centres. As can be seen in Figure 17 and 18 new low-pressure centres move in over and around Iceland during the studied period and with their anticlockwise wind-circulation they can transport volcanic ash into the Arctic. The arctic front is located at lower latitudes compared to the summer scenario and the polar dome has a larger extension compared to the previous scenario.

Init : Wed,08JAN2014 00Z Valid: Wed,08JAN2014 00Z  
 500 hPa Geopot. (gpm) und Bodendruck (hPa)

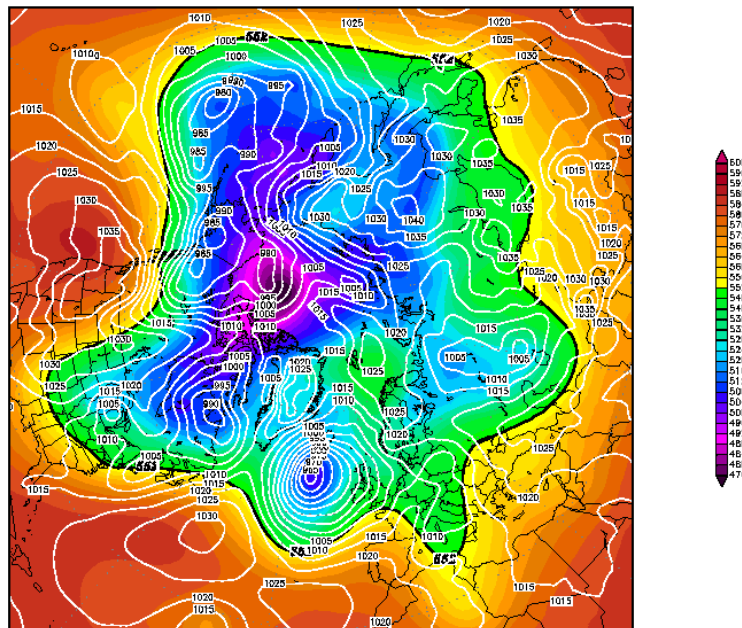


Daten: GFS-Modell des amerikanischen Wetterdienstes  
 (C) Wetterzentrale  
 www.wetterzentrale.de

**Figure 16.** The mean sea level pressure and the geopotential height for the 8<sup>th</sup> of January 2014 valid at 00 UTC (Wetterzentrale, 2014).



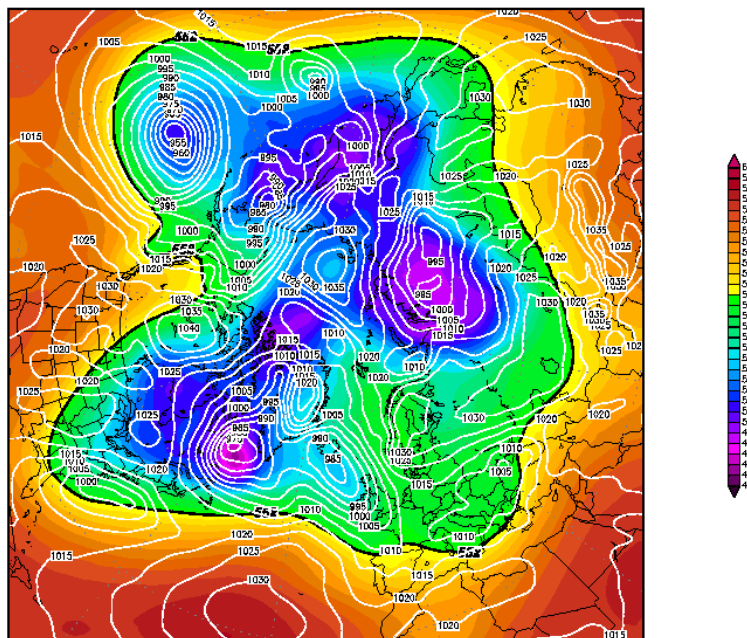
Init : Wed,15JAN2014 00Z Valid: Wed,15JAN2014 00Z  
 500 hPa Geopot. (gpm) und Bodendruck (hPa)



Daten: GFS-Modell des amerikanischen Wetterdienstes  
 (C) Wetterzentrale  
 www.wetterzentrale.de

Figure 17. The mean sea level pressure and geopotential height corresponding to the 17<sup>th</sup> of January 2014 valid at 00 UTC (Wetterzentrale, 2014).

Init : Wed,22JAN2014 00Z Valid: Wed,22JAN2014 00Z  
 500 hPa Geopot. (gpm) und Bodendruck (hPa)



Daten: GFS-Modell des amerikanischen Wetterdienstes  
 (C) Wetterzentrale  
 www.wetterzentrale.de

Figure 18. The mean sea level pressure and geopotential height for the 24<sup>th</sup> of January 2014 valid at 00 UTC (Wetterzentrale, 2014).

The dispersion of volcanic ash at a height of 2 m corresponds well to the wind pattern that is a result of the anticlockwise circulation due to the low-pressure centre west of Iceland. The atmospheric circulation created by the low-pressure centre transports the volcanic ash into the Arctic, as seen on the left in Figure A2:5.

At a height of 2 km the dispersion of ash has the appearance displayed in Figure A2:6. The initial plume moves towards the north over the Arctic and as the dispersion continues the ash particles become more evenly distributed and covers a larger geographical area, as seen on the right in Figure A2:6.

The volcanic ash particles dispersed at a height of 5 km are mainly located over the Arctic (see Figure A2:7).

The dispersion of ash at a height of 10 km is dominated by dispersion both towards and inside the Arctic region and the concentration is highest at the start of the studied period and becomes more uniform with time, (Figure 19). The maximum of the instantaneous concentration of volcanic ash particles is  $0.01 \text{ g/m}^3$  (see Figure 19).

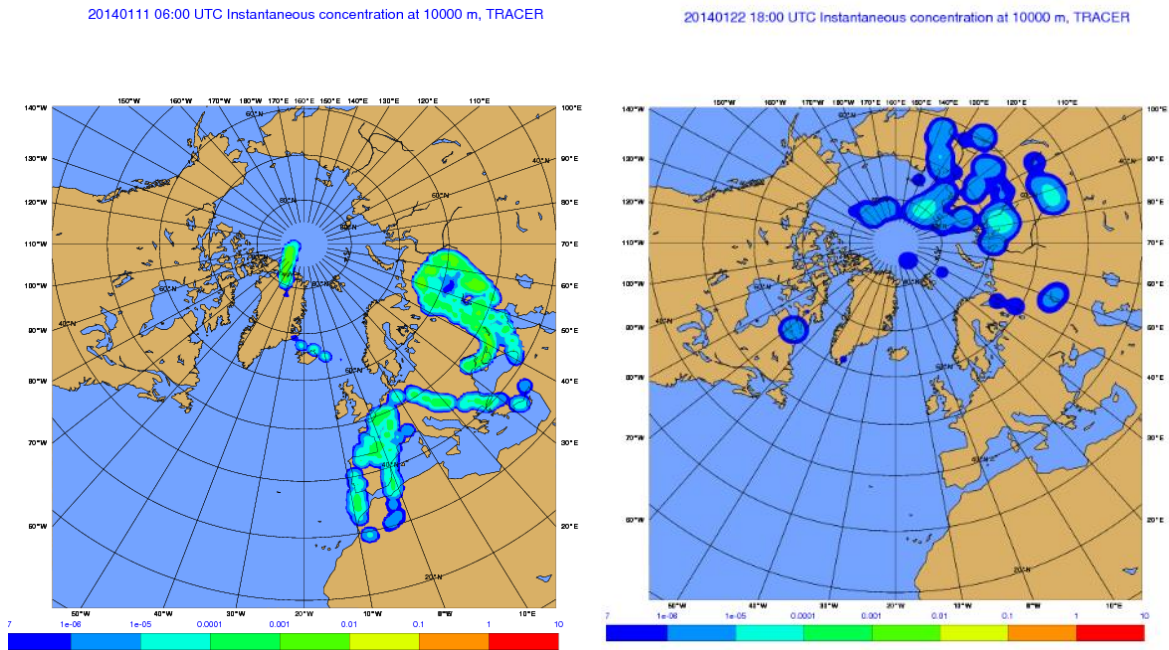


**Figure 19.** The instantaneous concentration of volcanic ash in  $\text{g/m}^3$  at a height of 10 km on the 11<sup>th</sup> and 22<sup>nd</sup> of January 2014 at 06 UTC respectively 18 UTC, as modelled by the help of DERMA.

As can be seen in Figure A2:8, the dispersion of volcanic ash particles at a height of 15 km is scarce over the entire Northern Hemisphere due to the height of the eruption plume that is mainly lower than 15 km.

The polar jet stream depicted in Figure 20 corresponds to the same point in time as the left part of Figure 19. When comparing the left part of Figure 19 and Figure 20, it is clear that the dispersion of volcanic ash at the northern coast of Greenland corresponds well to the southerly wind of the polar jet stream, situated in the region around Iceland and Greenland. The typical meandering pattern of the polar jet stream is displayed further south, see Figure 20.

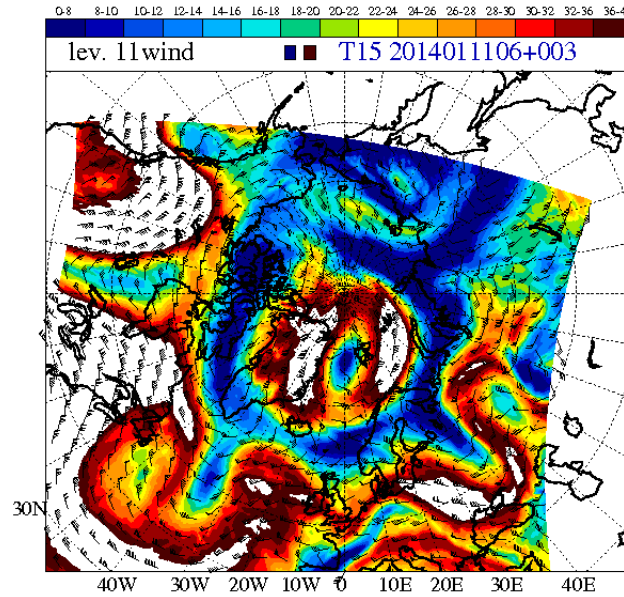


**Figure 20.** The wind pattern and the location of the polar jet stream on the 11<sup>th</sup> of January 2014 (MetGraf, 2014). The white colour indicates a greater wind velocity than the attached scale displays.

The precipitation in the Arctic region for the winter scenario is scarce, however the overall precipitation in the Northern Hemisphere is marginally higher, seen in Figure 21. The amount of precipitation depicted in Figure 21 is representative for the entire winter scenario.

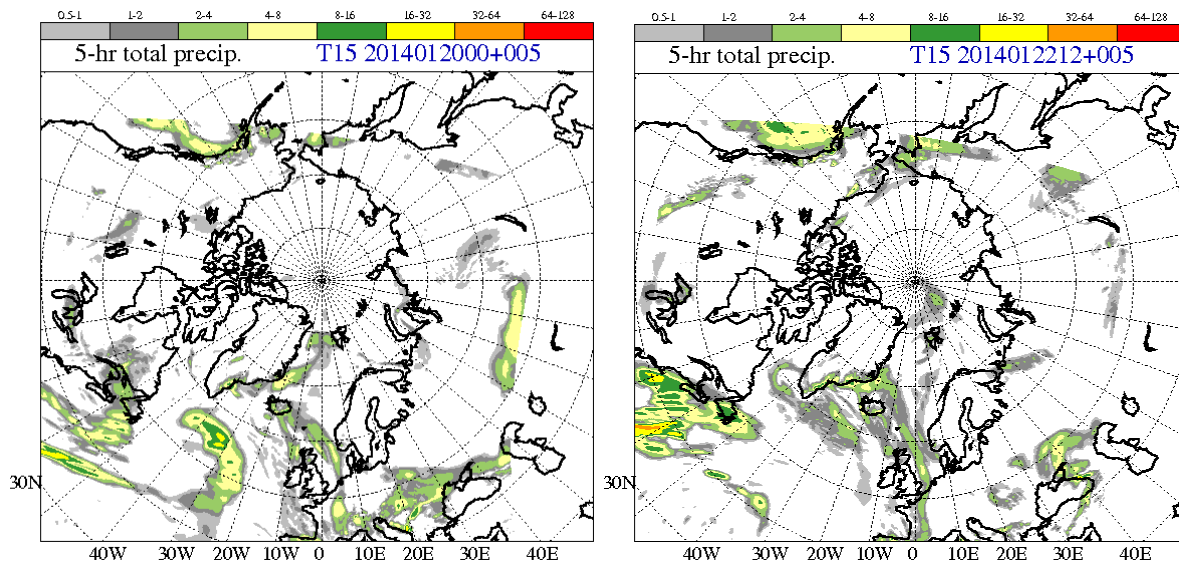


**Figure 21.** The 5-hour accumulated precipitation for the 20<sup>th</sup> and 22<sup>nd</sup> of January 2014 valid at 05 UTC respectively 17 UTC (MetGraf, 2014).

Deposition of volcanic ash during the winter period in 2014 is significant and cover large parts of the Northern Hemisphere and the Arctic, as seen in Figure 22. On Greenland the deposition of volcanic ash exceeds 1 g/m<sup>2</sup> and the deposition is on an average higher in the Arctic than in Europe.



20140122 18:00 UTC Total deposition at 0 m, TRACER

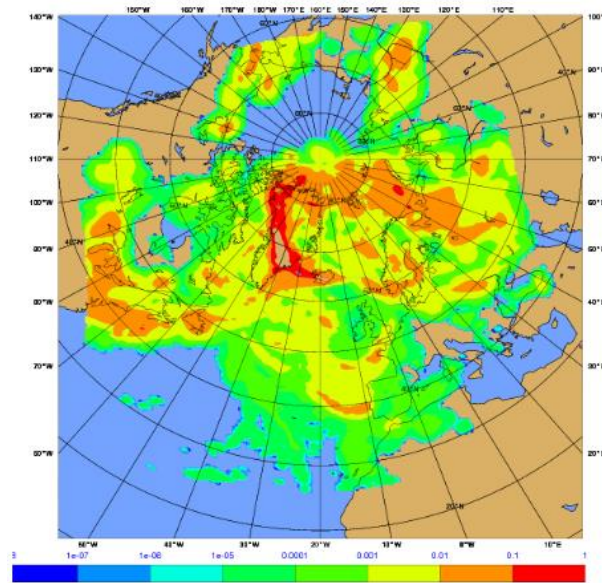


**Figure 22.** The total deposition of volcanic ash in  $\text{g/m}^2$  in the Northern Hemisphere during the studied two week period. The calculated deposition is a result of the DERMA model and the input data described in the method.

As the amount of volcanic ash emitted from the 2011 eruption of Grímsvötn was relatively moderate, a new scenario for the 2014 case was run by the help of DERMA. In the new scenario the plume height was multiplied by a factor of 1.5, (see Figure 23) and the eruption rate adjusted accordingly (Mastin et al., 2009), to be able to explore a larger eruption (see Figure 24). The increase in eruption rate with plume height according to Mastin et al. (2009) is followed as expected.

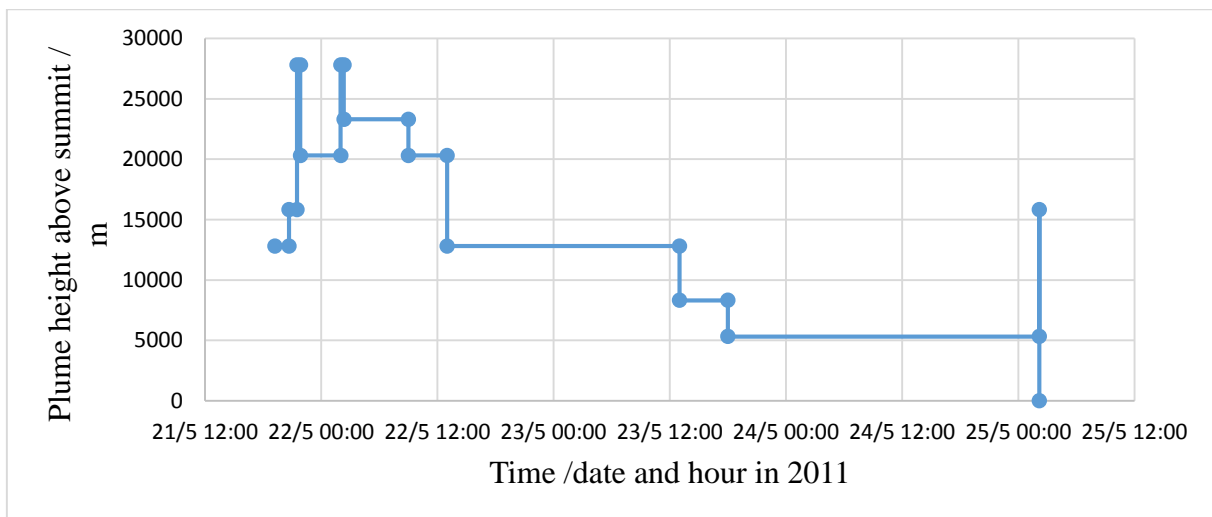


**Figure 23.** The increased source parameter alters the height of the ash plume by a factor 1.5. The data for the height of the ash plume is obtained from UK Met Office (2011).

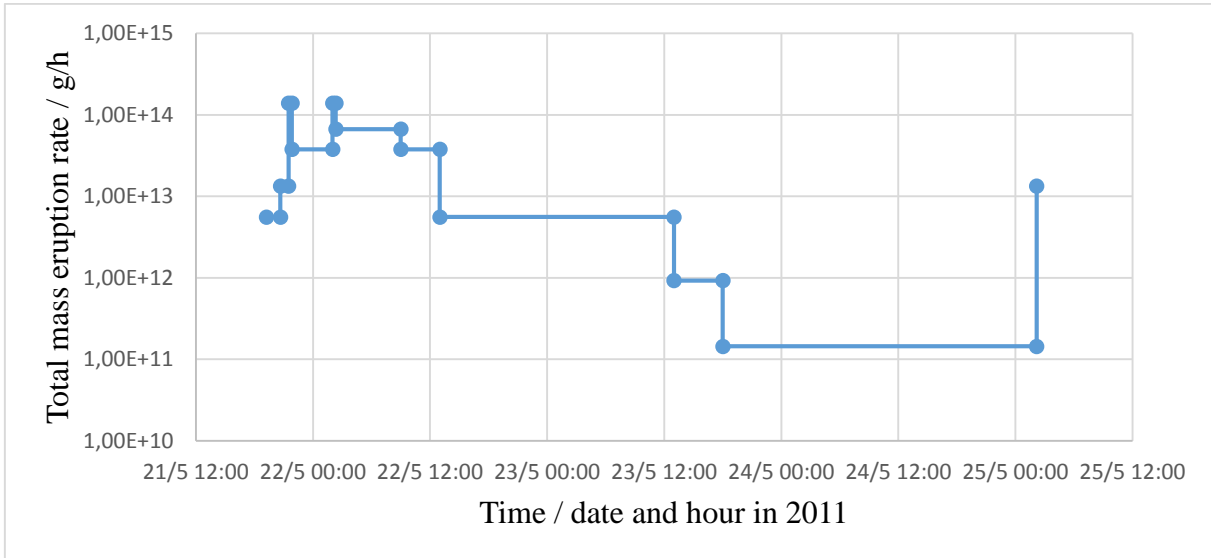


**Figure 24.** The eruption rate in g per hour for an increased source parameter by a factor of 1.5. The original data is obtained from UK Met Office (2011) and manipulated by the additional factor of 1.5.

The deposition for a more severe eruption is displayed in Figure 25; observe that the scale is a factor of 10 larger compared to the previous cases. The maximum deposition occurs at the same place as the previous case as it is the same meteorological case. However, the deposition of volcanic ash particles has increased by nearly a factor of 10, giving the highest deposition depicted to 10 g/m<sup>2</sup>.

20140122 18:00 UTC Total deposition at 0 m, TRACER

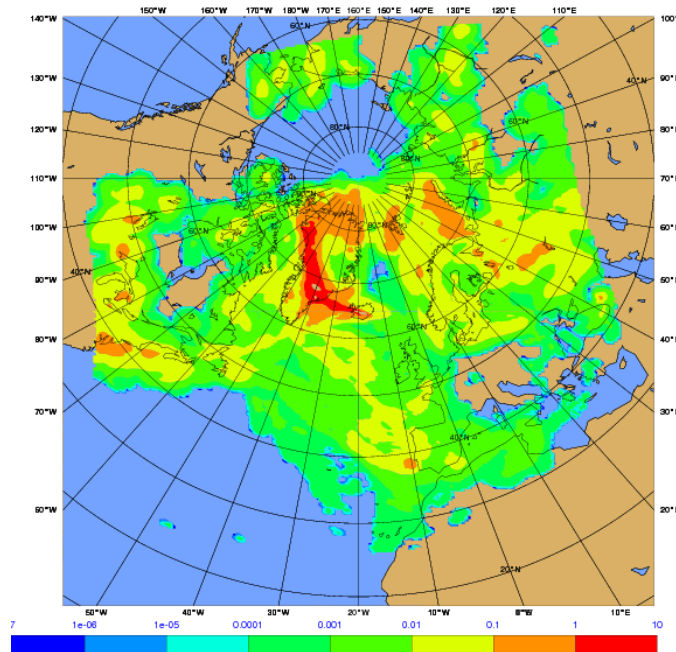


**Figure 25.** The total deposition of volcanic ash for an increase of the height of the ash plume by a factor of 1.5. Note that the legend is changed by a factor of 10 compared to Figure 22.

### **4.3 The atmospheric circulation and deposition of ash particles**

As expected the summer of 2006 is dominated by high-pressure centres around and inside the Arctic that is represented by a clockwise circulation, while the winter of 2014 is represented by multiple low-pressure centres in the Arctic region. As illustrated in Figures 9, 10 and 11 the ash is by the clockwise high-pressure circulation transported from Iceland to Europe and the Mediterranean in the summer of 2006. The southerly transport is a result of both the high-pressure centres, but also the location of the polar dome and the polar jet stream. As the polar dome is small and does not extend over Iceland it is difficult for the ash particles to be dispersed into the Arctic and the high-latitude position of the jet stream also makes the transport of ash into the Arctic more unlikely. However, in the winter of 2014 the atmospheric circulation is dominated by anticlockwise low-pressure circulation around Iceland making it more likely for the ash particles to be dispersed into the Arctic. Iceland is also situated inside the polar dome making it easier for the ash particles to be dispersed inside the dome than out of it. As the polar jet stream has a more southerly position in the winter of 2014 it also aides the ash particles to be dispersed in the Arctic. The results illustrate a possible difference in the seasonal dispersion of volcanic ash. However to accurately claim a seasonal dispersion, statistics need to be carried out for a large number of cases.

The total integrated deposition of ash particles is calculated by the use of integrals in DERMA and the difference between the deposition in 2006 compared to 2014 is significant. The total deposition in 2006 is  $3.9 \cdot 10^{12}$  g, the wet deposition is  $2.6 \cdot 10^{12}$  g and the dry deposition is  $1.3 \cdot 10^{12}$  g. The overall deposition of ash in 2014 is lower and the total deposition is  $1.1 \cdot 10^{12}$  g. The wet deposition in 2014 is  $9.4 \cdot 10^{11}$  g and the dry deposition is  $1.6 \cdot 10^{11}$  g. The difference in deposition of volcanic ash between the two periods is due to the different meteorological conditions of the areas of deposition. The dry deposition in the Arctic region in 2014 is significantly smaller, nearly a factor of 10, than the dry deposition in Europe in 2006. This difference is a result of the high static stability and low vertical mixing in the cold arctic conditions compared to the low static stability and highly convective conditions in Europe during summer.

The precipitation in the Arctic is normally low, as depicted in Figure 14 and 21, as it is a subduction zone. The conditions of subsidence contributes to a low wet deposition. As the European ground is warm in summer the air rises and cools, which produces precipitation that contributes to the wet deposition. As the vertical mixing is larger in summer in Europe and the Mediterranean the difference between the two types of deposition reduces during summer.

The total deposition is low in the winter of 2014 indicating that much volcanic ash is still airborne after two weeks and thereby transported away from the Arctic and deposited elsewhere. The deposition of ash is high in parts of Greenland in 2014 and when comparing the precipitation pattern with the area of deposition, it is seen that they correspond well. The good overlap illustrates that wet deposition is of great importance during the winter time in the Arctic as the static stability is high.

The total deposition for the enlarged scenario is  $4.0 \cdot 10^{12}$  g and the wet deposition is  $3.4 \cdot 10^{12}$  g, making the dry deposition  $6.0 \cdot 10^{11}$  g. The total deposition is roughly a factor of 4 greater compared to the previous winter case. Apart from the circulation pattern, the deposition is highly dependent on the size of the eruption as shown by the different amount of deposition in the two cases in 2014. The difference between the wet and dry deposition is greater in the enlarged scenario making the feature of a low vertical mixing in winter more evident.

#### 4.4 The effect on air traffic

The dispersion of ash at 10 km is highly dependent on the polar jet stream and it can be seen clearly in Figure 12 and 13 how the dispersion of ash particles corresponds well with the position of the polar jet stream. The strength of the polar jet stream is higher in the winter of 2014 compared to the summer of 2006 due to larger temperature differences between high- and low latitudes in wintertime. The position of the polar jet stream is expected to be at lower latitudes in winter compared to summer. However this expected pattern is not clearly shown by Figure 19 and 20 due to the constant meandering of the jet stream.

The maximum concentration of ash particles at a height of 10 km is  $10 \text{ mg/m}^3$  both in 2006 and 2014, as seen in Figure 12 and 19, and thereby the concentration exceeds the recommendation of good flying conditions. However the location of the ash particles is different and therefore giving problems for different air routes. In 2014 the concentration is high over the southeast coast of Greenland and poses a risk to the air traffic between Europe and the United States, as the air traffic route passes over Greenland. The period of such a high concentration is however very short and most likely does not mean any prolonged restrictions on the air traffic. Nevertheless it can result in delays of certain flights. In 2006 there is a high concentration of ash particles over Europe. However, this period of high concentration is also short and will not significantly affect the approximately 20,000 daily flights in the European airspace.

#### 4.5 The impact on snow and ice albedo

The thickness of the deposited ash layer can be calculated by using the following equations

$$A \cdot h \cdot \rho = m \quad (1)$$

$$h = \frac{m}{A} \cdot \frac{1}{\rho} \quad (2)$$

$$h = d \cdot \frac{1}{\rho} \quad (3)$$

where  $A$  is the area covered by the ash layer,  $h$  is the thickness of the layer,  $\rho$  is the ash density in  $\text{kg/m}^3$  and  $d$  is the deposition in  $\text{kg/m}^2$ .

The density of the ash layer is approximately  $500\text{-}1500 \text{ kg/m}^3$ , however this is highly dependent on the compaction of the volcanic ash particles (USGS, 2009). The density for the ash layer used in this project is more likely closer to  $500 \text{ kg/m}^3$ , since it is dry and relatively new fallen. The deposition of ash is only of interest for the largest deposition values (red area, see

Figure 15), namely between 0.1 to 1 g/m<sup>2</sup>. This gives a thickness of the ash layer to 0.2 – 2 µm, by the use of Equations (1)-(3). The thickness of the deposited ash layer is very low and at present there is a lack of knowledge in the effect of such thin ash layers. To increase the knowledge of the effect of thin layers of volcanic ash more field measurements need to be carried out and assessed.

The deposition of ash particles is at a maximum of 1 g/m<sup>2</sup> for the summer of 2006, while the deposition exceeds this value at Greenland during the winter of 2014. Figure 3 and Table 1 indicate that the reduction of albedo with a deposition of 16.7 g/m<sup>2</sup> is 30 % and as the deposition in this case is a factor of 10 lower, the impact on albedo is probably insignificant. Therefore the deposition of ash particles, due to the 2011 eruption of Grímsvötn, will not have a significant effect on the radiative properties of the atmosphere and the long- and short-term climate in the Arctic in the cases considered.

The highest value for the deposition of ash particles in 2014 with an increased source term is 10 g/m<sup>2</sup>. The deposition with the increased plume height is fairly close to the value of 16.7 g/m<sup>2</sup> that corresponds to a 30 % reduction of the albedo. It is therefore possible that the high deposition can lead to a reduction of the snow and ice albedo and cause snow and ice melt and thereby also short- term effects on the climate.

If the ash particles create cryoconite holes, the impact on the snow and ice albedo can be significant and short-term effects on the climate can be visible. If cryoconite holes are created they reduce the albedo of the ice sheet and result in short-term ice loss. However the dark matter will after some time be covered by new ice and snow and the effect on the albedo is lost, as well as the short-term climate effect.

It can be argued that the climatic effect due to changes in snow and ice albedo by volcanic ash possibly is larger in winter time due to the larger extent of the ice sheet. The results illustrate that, with respect to the Arctic, it is better if an eruption takes place in the summer compared to the winter. However, concerning the air traffic over Europe, an eruption in summer has more complications than an eruption in winter would have.

#### **4.6 Future outlook of Arctic research**

As the Arctic region is getting warmer and has shown the highest warming effects globally, future research on Arctic climate is vital to halt the alarming development (NSIDC, 2014d). The warming of the region causes the arctic sea ice extent to shrink, as well as the snow and ice cover and the extent of the permafrost (NSIDC, 2014d). The climate changes occurring in the Arctic are of great importance for the entire globe, since the Arctic region functions as a global cooling system as the region gives off more heat than it absorbs and redistributes cool air (NSIDC, 2014d).

The research of the atmospheric circulation and the deposition of particles on ice and snow covered surfaces in the Arctic is incomplete and scarce. Therefore the aim of future research should be to increase the knowledge of these factors as they can affect the future of Arctic and

global climate. It is important to have a good understanding of the effect of particles and gases on ice and snow covered surfaces since such parameters can affect the albedo and are also important input parameters in climate models. Without a good sense of how these processes work, the future climate cannot be predicted in models in a reasonable manner. As well as affecting climate modelling, the deposition of particles and gases in the Arctic ought to receive more attention in the future as the deposition of particles have the potential to affect the ice cover and the melting process of it. Since the ice cover on Greenland is currently melting the sea level is rising and if the entire ice cover melts the sea level can rise by as much as 6.5 meters (Benn and Evans, 2010). Therefore the effect of particles on ice and snow-covered surfaces are of great importance for the future.

## **5. Summary**

The results indicate a possible seasonal circulation pattern to and inside the Arctic. The atmospheric circulation illustrates a winter circulation from Iceland to the Arctic, while the circulation is towards Europe and the Mediterranean in the summer. The deposition of volcanic ash is significantly larger in the summer of 2006 compared to the winter of 2014. The reason for the difference in deposition is the high static stability and low vertical mixing in the Arctic during winter compared to the low static stability and highly convective conditions in Europe during summer.

The deposition of volcanic ash in the Arctic is not sufficiently large to claim an effect on the climate as the research on thin ash layers is scarce. As the eruption size increases the deposition of volcanic ash also shows an increase, leading to the conclusion that a larger eruption might affect the radiation balance and albedo of the ice cover in the Arctic. The effect on air traffic by the 2011 eruption of Grímsvötn is not great in the cases considered, since the concentration of ash particles only exceeds the restriction value for good flying conditions for short periods of time. The result of the airborne ash particles is most likely only delays of a few departures.

## 6. References

- ACIA. (2005). *Arctic Climate Impact Assessment*. Cambridge University Press.
- Agency for Toxic Substances and Disease Registry (ATSDR). (2003). *Toxicological profile for Fluorides, Hydrogen Fluoride, and Fluorine*. U.S. Department of Health and Human Services, Public Health Service.
- Ahrens, C. D. (2013). *Meteorology Today: An Introduction to Weather, Climate, and the Environment*. 10<sup>th</sup> edition. Brooks/Cole.
- Anesio, A. M., Hodson, A. J., Fritz, A., Psenner, R. and Sattler, B. (2009). *High microbial activity on glaciers: importance to the global carbon cycle*. *Global Change Biology* 15, 955–960. doi: 10.1111/j.1365-2486.2008.01758.x
- Arctic Council. (2009). *Arctic Marine Shipping Assessment 2009 Report (AMSA)*. 2<sup>nd</sup> edition. Arctic Council.
- Barrie, L. A. (1986). *Arctic air pollution – An overview of current knowledge*. *Atmospheric Environment*, 20:643-663.
- Benn, D. and Evans D. (2010). *Glaciers & Glaciation*. 2<sup>nd</sup> edition. Hodder Arnold Publication.
- Bøggild Egede, C., Brandt, R. E., Brown, K. J. and Warren, S. G. (2010). *The ablation zone in northeast Greenland: ice types, albedos and impurities*. *Journal of Glaciology* 56, 195.
- Carlson, T. N. (1981). *Speculations on the movement of polluted air to the Arctic*. *Atmospheric Environment*, 15:1473-1477.
- Civil Aviation Authority, (CAA). (2014). *Managing ash in UK air space*. Accessed 14 April 2014 at <http://www.caa.co.uk/default.aspx?catid=2011&pagetype=90&pageid=12639>.
- Conway, H., Gades, A. and Raymond, C. F. (1996). *Albedo of dirty snow during conditions of melt*. *Water Resources Research* 32, 1713-1718.
- Cook, J. and Box, J. (2014). *Ice Sheet Microbes and Melt: Dark Snow 2014*. Accessed 25 April at <http://tothepoles.wordpress.com/2014/04/22/ice-sheet-microbes-and-melt-dark-snow-2014/>.
- Corell, R. W. (2006). *Challenges of Climate Change: An Arctic Perspective*. *Ambio*, 35: 4.
- Cuffey, K. M. and Paterson, W. S. B. (2010). *The physics of glaciers*. 4<sup>th</sup> edition. Academic Press.
- Duggen, S., Olgun, N., Croot, P., Hoffmann, LDH. and Teschner, C. (2009). *The role of airborne volcanic ash for the surface ocean biogeochemical iron-cycle: a review*. *Biogeosciences Discussions* 6: 6441-6489.



Durant, A. J., Bonadonna, C. and Horwell C. J. (2010). *Atmospheric Particles: Atmospheric and Environmental Impacts of Volcanic Particulates*. ELEMENTS, (4): 235-240. doi: 10.2113/gselements.6.4.235

Guenther, A. and Lamb, B. (1989). *Atmospheric dispersion in the Arctic: Winter-time boundary-layer measurements*. Laboratory for Atmospheric Research, Washington State University.

Hansen, B. S. (2014). *DMI-HIRLAM*. Danmarks Meteorologiske Institut. Accessed 15 April 2014 at <http://www.dmi.dk/laer-om/temaer/meteorologi/hirlam/>.

Heidam, N. Z., Christensen, J., Wåhlin, P. and Skov, H. (2004). *Arctic atmospheric contaminants in NE Greenland: levels, variations, origins, transport, transformations and trends 1990-2001*. Science of The Total Environment 331, 5-28.

Higuchi, K. and Nagoshi, A. (1977). *Effect of particulate matter in surface snow layers on the albedo of perennial snow patches*. LAHS AISH public 118, 95-97.

Iversen, T. (1984). *On the atmospheric transport of pollution to the Arctic*. Geophysical Research Letters, 11:457-460.

Keller, E. A. and DeVecchio, D. E. (2012). *Natural Hazards – Earth's processes as hazards, disasters and catastrophes*, 3<sup>rd</sup> edition. New Jersey: Pearson Education, Inc.

Klonecki, A., Hess, P., Emmons, L., Smith, L., Orlando, J. and Blake, D. (2003). *Seasonal changes in the transport of pollutants into the Arctic troposphere – Model study*. Journal of Geophysical Research, 108(D4):8367.

Korsholm Smith, U., Astrup, P., Lauritzen, B. and Sørensen Havskov, J. (2011). *NKS NordRisk II: Atlas of long-range atmospheric dispersion and deposition of radionuclides from selected risk sites in the Northern Hemisphere*. Denmark: Danish Meteorological Institute (DMI) and Risø DTU (Technical University of Denmark).

Korsholm Smith, U. (2014). *Oral discussion on 7 May 2014*. Denmark: Danish Meteorological Institute, DMI.

Mastin, L. G., Guffanti, M., Servranckx, R., Webley, P., Dean, K., Durant, A., Ewert, J. W., Neri, A., Rose, W. I., Schneider, D., Siebert, L., Stunder, B., Swanson, G., Tupper, A., Volentik, A. and Waythomas, C. F. (2009). *A multidisciplinary effort to assign realistic source parameters to models of volcanic ash-cloud transport and dispersion during eruptions*. Journal of Volcanology and Geothermal Research 186, 10-21. doi: 10.1016/j.jvolgeores.2009.01.008

National Snow and Ice Data Center, (NSIDC). (2014a). *Factors Affecting Arctic Weather and Climate*. Accessed 02 April 2014 at [http://nsidc.org/cryosphere/arctic-meteorology/factors\\_affecting\\_climate\\_weather.html](http://nsidc.org/cryosphere/arctic-meteorology/factors_affecting_climate_weather.html)

- National Snow and Ice Data Center, (NSIDC). (2014b). *Patterns in Arctic climate and weather*. Accessed 02 April 2014 at [http://nsidc.org/cryosphere/arctic-meteorology/weather\\_climate\\_patterns.html](http://nsidc.org/cryosphere/arctic-meteorology/weather_climate_patterns.html).
- National Snow and Ice Data Center, (NSIDC). (2014c). *What is the Arctic?* Accessed 07 April 2014 at <https://nsidc.org/cryosphere/arctic-meteorology/arctic.html>.
- National Snow and Ice Data Center, (NSIDC). (2014d). *Climate change in the Arctic*. Accessed 08 April 2014 at [https://nsidc.org/cryosphere/arctic-meteorology/climate\\_change.html](https://nsidc.org/cryosphere/arctic-meteorology/climate_change.html).
- Niemeier, U., Timmreck, C., Graf, H. F., Kinne, S., Rast, S. and Self, S. (2009). *Initial fate of fine ash and sulfur from large volcanic eruptions*. *Atmospheric Chemistry and Physics* 9, 9043-9057.
- Nuttall, M. and Callaghan, T. V. (2000). *The Arctic – Environment, People, Policy*. Amsterdam: Harwood academic publishers.
- Petersen GN., Bjornsson H., Arason P, and von Löwis S. (2012). *Two weather radar time series of the altitude of the volcanic plume during the May 2011 eruption of Grímsvötn, Iceland*. *Earth System Science Data* 4(1): 121–127. doi:10.5194/essd-4-121-2012.
- Przyborski, P. (2011). *Eruption of Grímsvötn Volcano, Iceland*. NASA – Earth Observatory. Accessed: 02 April 2014 at <http://earthobservatory.nasa.gov/NaturalHazards/view.php?id=50684>.
- Runólfsson, H. (2010). *Guidelines for livestock owners in areas where there is downfall of volcanic ash*. Accessed 11 May 2014 at <http://www.mast.is/Uploads/document/leidbeiningar/Enska/downfalofashguidelines.pdf>.
- Quinn, P.K., Stohl, A., Arneth, A., Berntsen, T., Burkhardt, J. F., Christensen, J., Flanner, M., Kupiainen, K., Lihavainen, H., Shepherd, M., Shevchenko, V., Skov, H. and Vestreng, V. (2011). *The Impact of Black Carbon on Arctic Climate*. Oslo: Arctic Monitoring and Assessment Programme (AMAP) Technical Report No. 4.
- Rodionov, S. N., Bond, N. A. and Overland, J.E. (2007). *The Aleutian Low, storm tracks, and winter climate variability in the Bering Sea*. *Deep-sea Research II* 54: 2560-2577. doi: 10.1016/j.dsr2.2007.08.002.
- Serreze, M. C., and R. G. Barry. (2005). *The Arctic Climate System*. 1<sup>st</sup> ed. Cambridge: Cambridge University Press. Cambridge Books Online. Accessed 02 April 2014. <http://dx.doi.org/10.1017/CBO9780511535888>
- Sigmarsson, O. (2012) *Mafic intrusions triggering eruptions in Iceland*. *Geophysical Research Abstracts* 14: EGU2012–12722.
- Sigurdsson, H. (1990). *Assessment of the atmospheric impact of volcanic eruptions*. Geological Society of America, 247.

Stevenson, J. A., Loughlin, S. C., Font A., G. W., MacLeod A., Oliver I. W., Jackson B., Horwell C. J., Thordarson T. and Dawson I. (2013). *UK monitoring and deposition of tephra from the May 2011 eruption of Grímsvötn, Iceland*. Journal of Applied Volcanology 2:3. doi:10.1186/2191-5040-2-3

Stohl, A. (2006). *Characteristics of atmospheric transport into the Arctic troposphere*. Journal of Geophysical Research, 111:D11306.

Strunin, M. A., Postnov, A. A. and Mezrin, M. Y. (1997). *Meteorological potential for contamination of arctic troposphere: Boundary layer structure and turbulent diffusion characteristics*. Atmospheric Research, 44:37-51.

Sørensen Havskov, J. (2014). *Oral discussion on 2 May 2014*. Denmark: Danish Meteorological Institute, DMI.

Sørensen Havskov, J., Baklanov., A. and Hoe, S. (2007). *The Danish emergency response model of the atmosphere (DERMA)*. Journal of Environmental Radioactivity 96, 122-129.

UK Met Office. (2014). *Volcano and dust monitoring*. Accessed at 08 April 2014 at <http://research.metoffice.gov.uk/research/nwp/satellite/imagery/aerosol.html>.

UK Met Office. (2011). *Source parameters used in the Met Office NAME model during the eruption of Grímsvötn in May 2011*. United Kingdom.

U.S. Geological Survey (USGS). (2009). *Ash properties and dispersal by the wind*. Accessed at 29 April 2014 at <http://volcanoes.usgs.gov/ash/properties.html>.

Vatnajökull National Park. (2014). *Grímsvötn*. Accessed 25 March 2014 at <http://www.vatnajokulsthjodgardur.is/english/education/grimsvotn/>.

Warren, S. G. and Wiscombe, W. J. (1985). *Dirty snow after nuclear war*. Nature 313, 467-470.

Woo, M. K. and Dubreuil, M. A. (1985). *Empirical relationship between dust content and arctic snow albedo*. Cold Regions Science and Technology 10, 125-132.

### Picture references

Ahrens, C. D. (2009). *Meteorology Today: An Introduction to Weather, Climate, and the Environment*. 9<sup>th</sup> edition. Brooks/Cole.

DMI logo. Accessed 15 April 2014 at <http://www.dmi.dk/om-dmi/presse/dmis-logo/>.

DMI. (2014). *The 40 vertical pressure levels of the HIRLAM model*. Received from Sørensen, J. H. at 15 April 2014.

Gustafson, M. (2011). *Oljeutvinning på hal is*. Accessed 6 May 2014 at <http://maxgustafson.se/2011/11/oljeutvinning-pa-hal-is/>.

Lund university logo. Accessed 08 April 2014 at <http://www.brandsoftheworld.com/logo/lund-university>.

Quinn, P.K., Stohl, A., Arneth, A., Berntsen, T., Burkhardt, J. F., Christensen, J., Flanner, M., Kupiainen, K., Lihavainen, H., Shepherd, M., Shevchenko, V., Skov, H. and Vestreng, V. (2011). *The Impact of Black Carbon on Arctic Climate*. Oslo: Arctic Monitoring and Assessment Programme (AMAP) Technical Report No. 4.

Wetterzentrale. (2014). *Archiv der AVN-Nordhemisphärenanalysen*. Accessed 22 April 2014 at <http://www.wetterzentrale.de/topkarten/fsavneur.html>.

## 7. Appendix

### 7.1 Appendix 1.

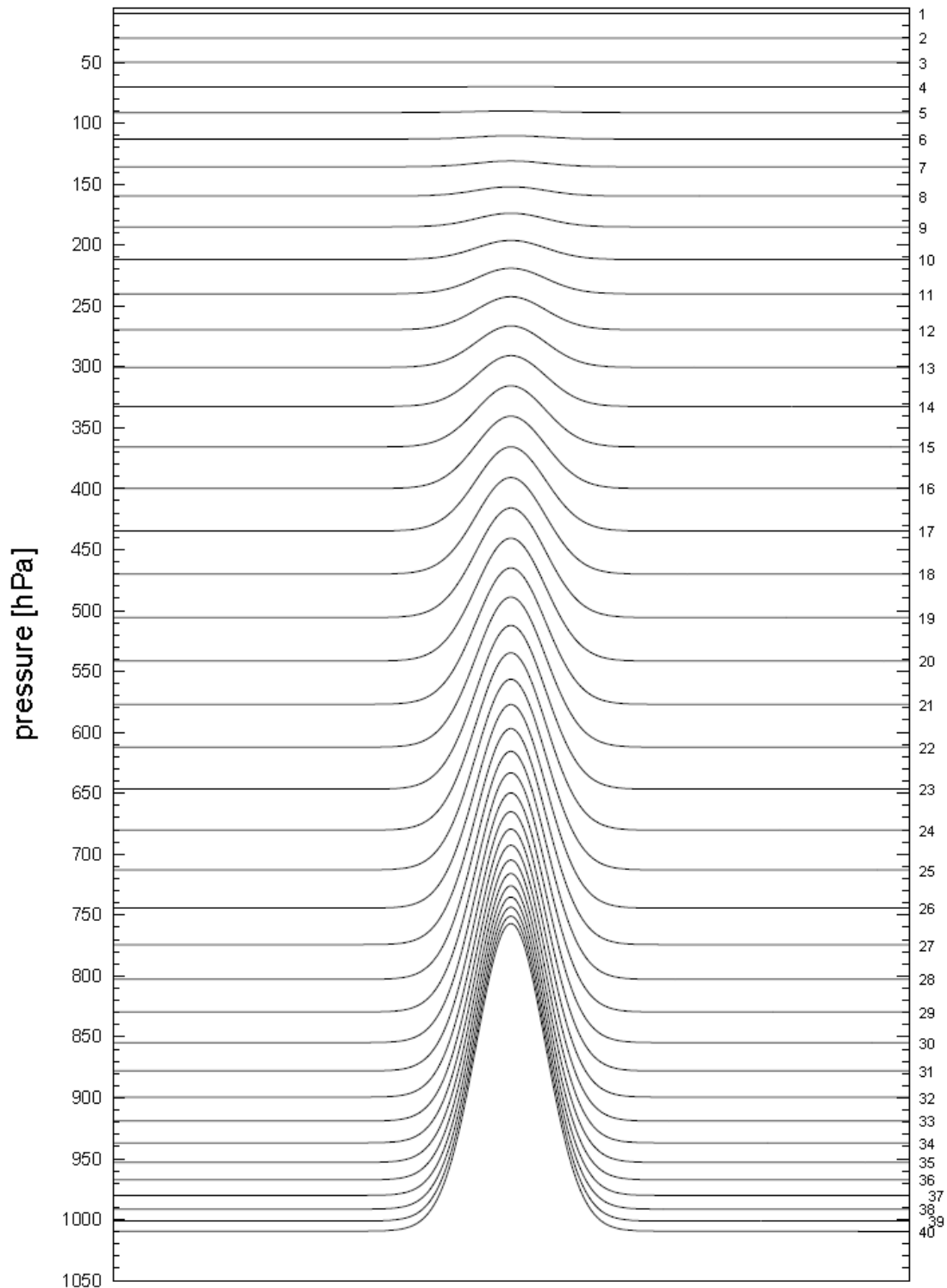


**Figure 21.** The 40 vertical levels of the HIRLAM T15 model covering a large part of the Northern Hemisphere (DMI, 2014). The levels are displayed using an average surface pressure of 1010 hPa. The x-axis should be seen as an illustration of the behaviour of the vertical coordinate, which is a hybrid coordinate, meaning that it behaves as a sigma-level close to the surface and as a pressure coordinate higher up in the modelled atmosphere.

7.2 Appendix 2.

20060818 12:00 UTC Instantaneous concentration at 2 m, TRACER

20060824 18:00 UTC Instantaneous concentration at 2 m, TRACER

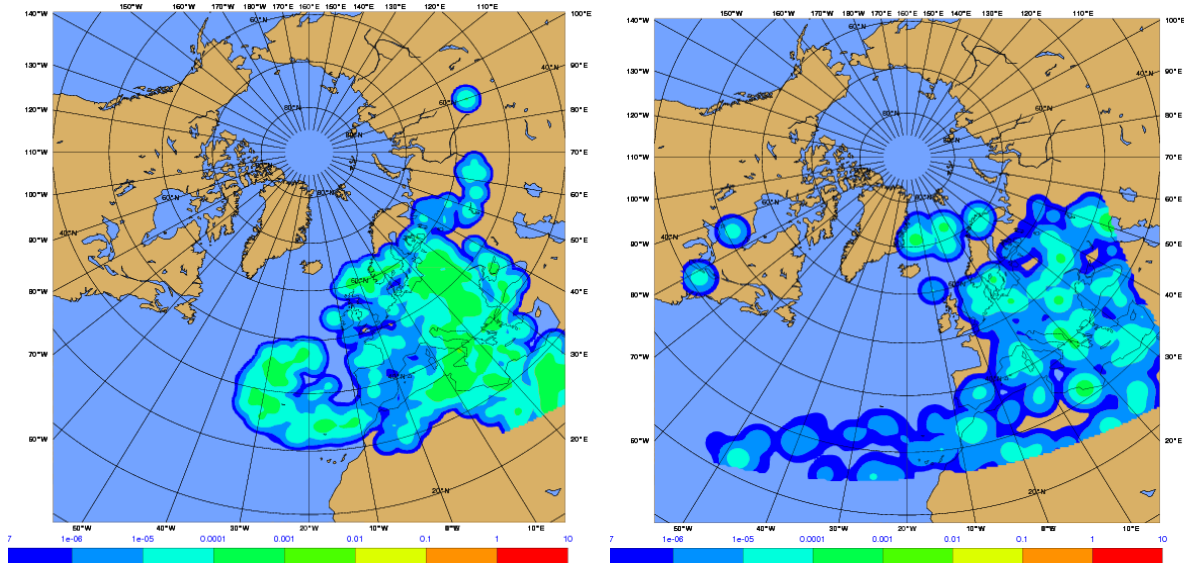


**Figure A2:1.** The instantaneous concentration of ash particles in  $g/m^3$  at 2 m above the surface on the 18<sup>th</sup> and 24<sup>th</sup> of August 2006 at 12 UTC respectively 18 UTC.

20060814 06:00 UTC Instantaneous concentration at 2000 m, TRACER

20060824 18:00 UTC Instantaneous concentration at 2000 m, TRACER

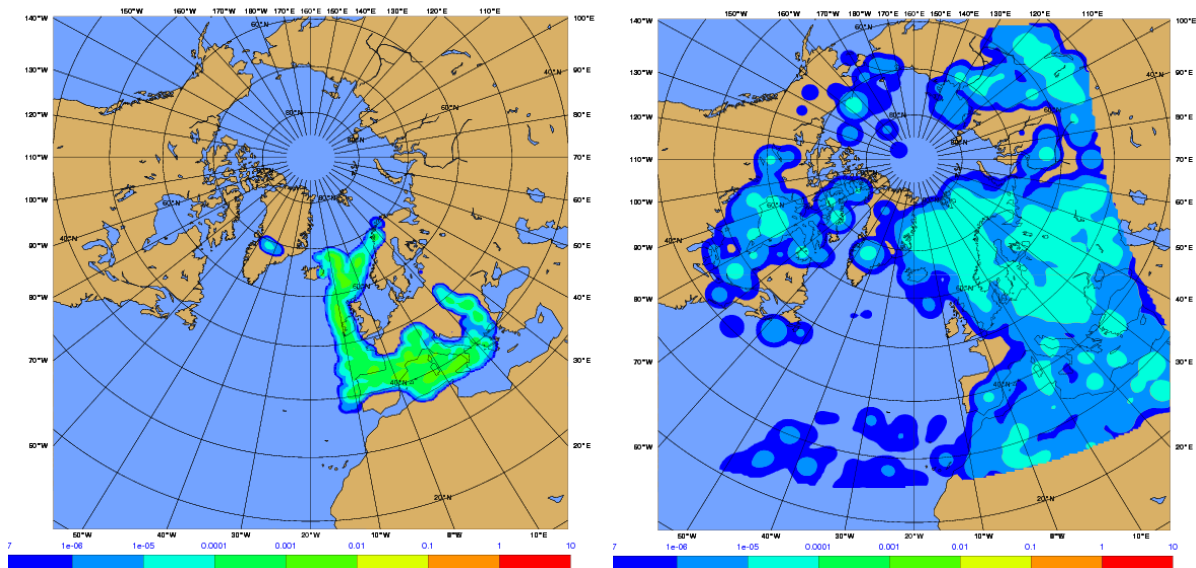


**Figure A2:2.** The instantaneous concentration of ash particles in  $g/m^3$  at 2 km on the 14<sup>th</sup> and 24<sup>th</sup> of August 2006 at 06 UTC respectively 18 UTC.



20060813 12:00 UTC Instantaneous concentration at 5000 m, TRACER

20060824 18:00 UTC Instantaneous concentration at 5000 m, TRACER

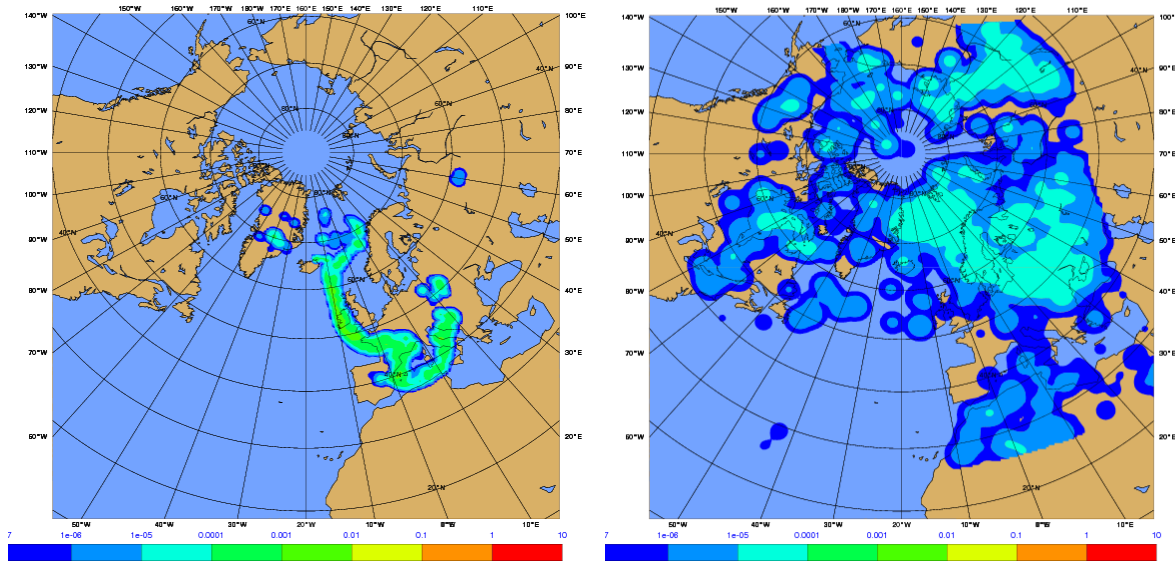


**Figure A2:3.** The instantaneous concentration of ash particles in  $\text{g/m}^3$  at 5 km on the 13<sup>th</sup> and 24<sup>th</sup> of August 2006 at 12 UTC respectively 18 UTC.

20060811 18:00 UTC Instantaneous concentration at 15000 m, TRACER

20060824 18:00 UTC Instantaneous concentration at 15000 m, TRACER

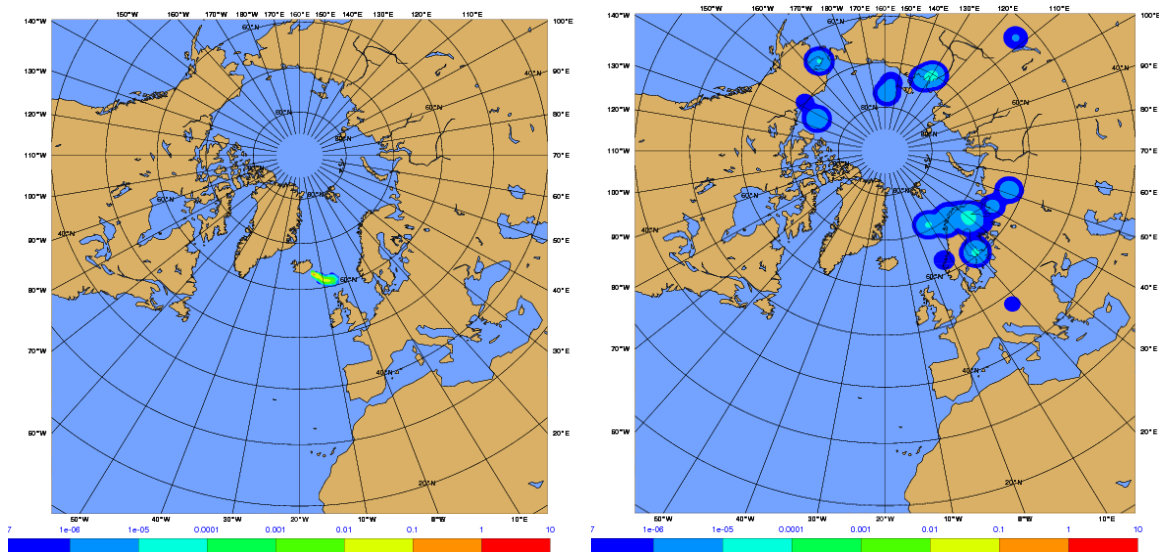


**Figure A2:4.** The instantaneous concentration of ash particles in  $\text{g/m}^3$  at 15 km on the 11<sup>th</sup> and 24<sup>th</sup> of August 2006 at 18 UTC in both cases.

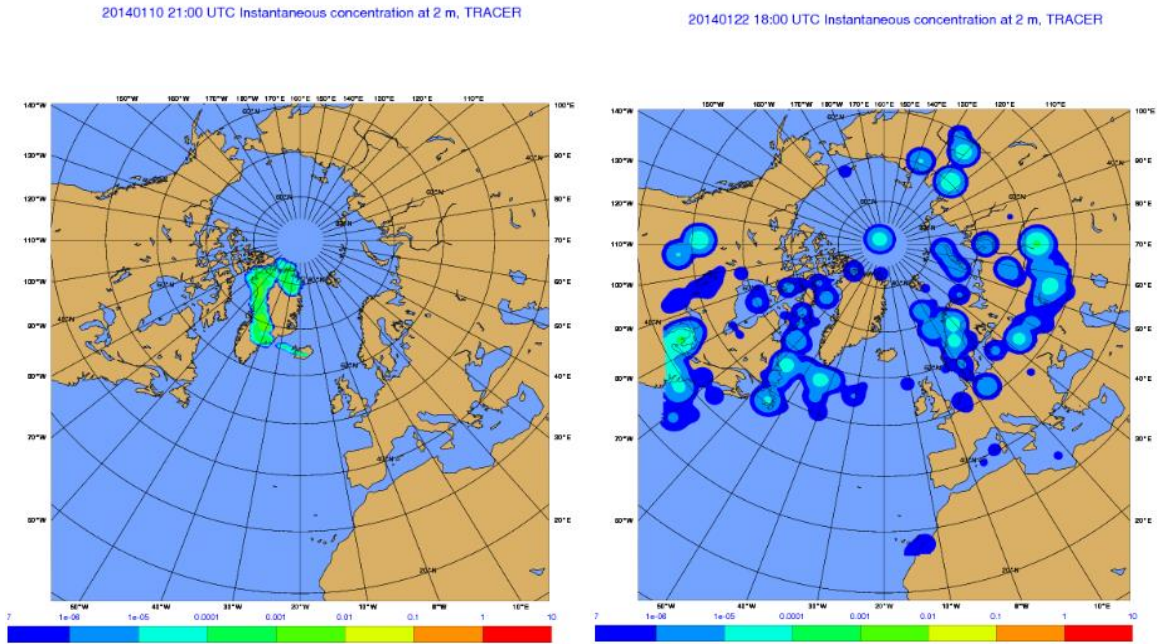


**Figure A2:5.** The instantaneous concentration of ash particles in  $\text{g/m}^3$  at 2 m on the 10<sup>th</sup> and 22<sup>nd</sup> of January 2014 at 21 UTC respectively 18 UTC.

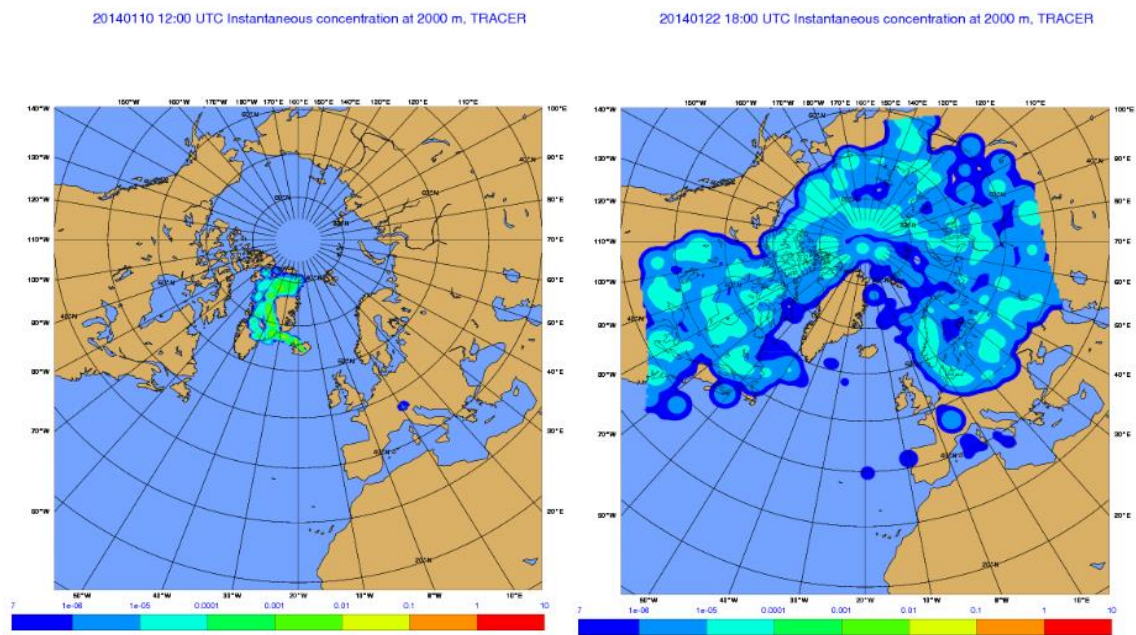


**Figure A2:6.** The instantaneous concentration of ash particles in  $\text{g/m}^3$  at a height of 2 km on the 10<sup>th</sup> and 22<sup>nd</sup> of January 2014 at 12 UTC respectively 18 UTC.



20140112 21:00 UTC Instantaneous concentration at 5000 m, TRACER

20140122 15:00 UTC Instantaneous concentration at 5000 m, TRACER

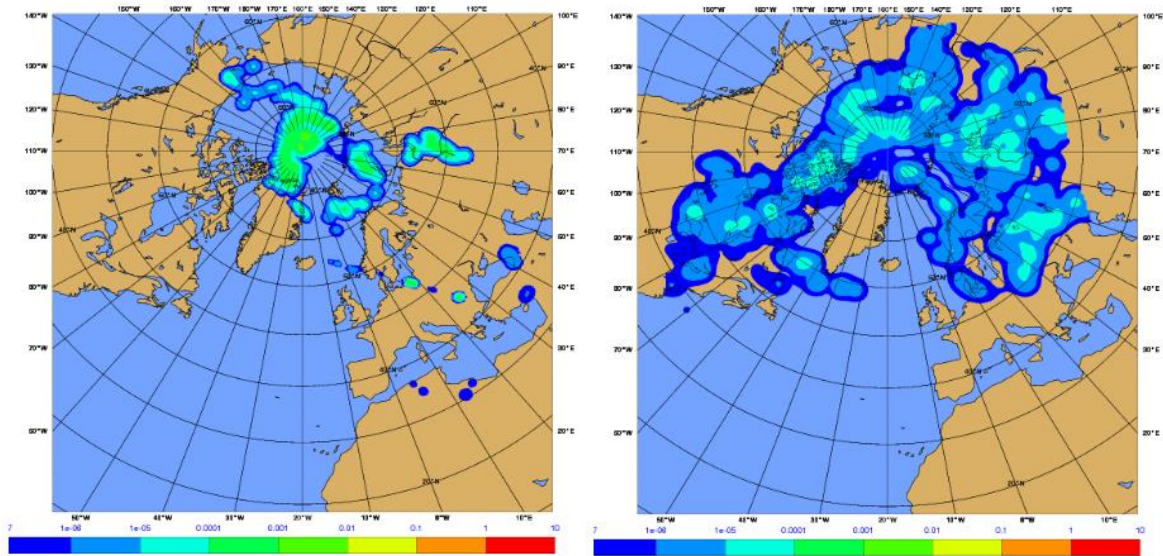


**Figure A2:7.** The instantaneous concentration of ash particles in  $\text{g/m}^3$  at 5 km on the 12<sup>th</sup> and 22<sup>nd</sup> of January 2014 at 21 UTC respectively 15 UTC.

20140109 18:00 UTC Instantaneous concentration at 15000 m, TRACER

20140122 18:00 UTC Instantaneous concentration at 15000 m, TRACER

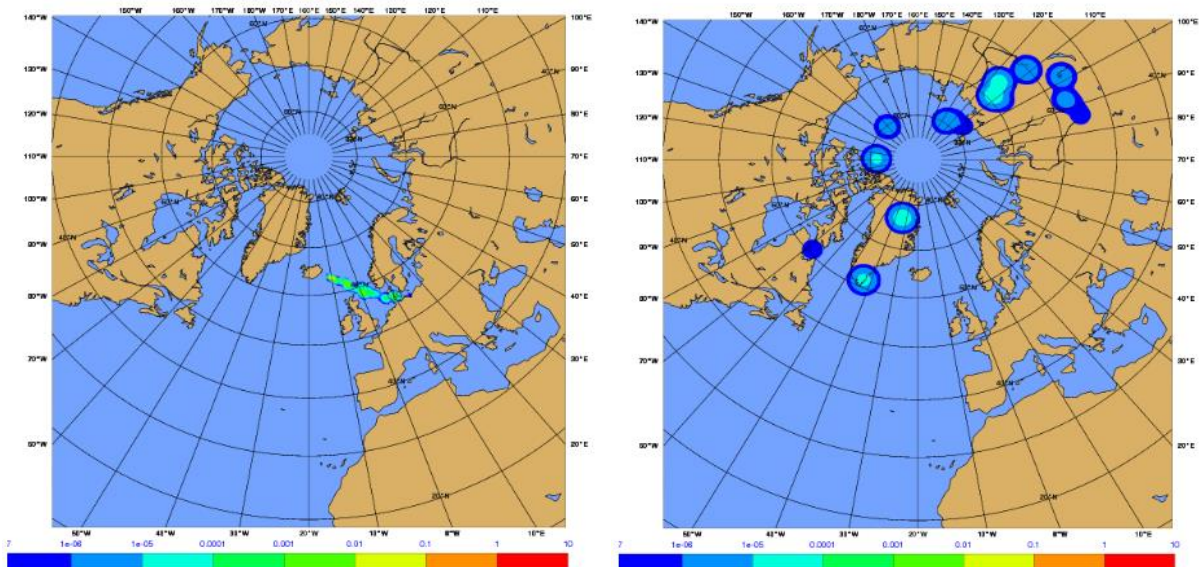


**Figure A2:8.** The instantaneous concentration of ash particles in  $\text{g/m}^3$  at 15 km on the 9<sup>th</sup> and 22<sup>nd</sup> of January 2014 at 18 UTC in both cases.